

Complementary lattice arrays for coded aperture imaging

JIE DING,* MOHAMMAD NOSHAD, AND VAHID TAROKH

John A. Paulson School of Engineering and Applied Sciences, Harvard University, Cambridge, Massachusetts 02138, USA

*Corresponding author: jieding@fas.harvard.edu

Received 7 December 2015; revised 25 February 2016; accepted 1 March 2016; posted 9 March 2016 (Doc. ID 255120); published 15 April 2016

In this work, we propose the concept of complementary lattice arrays in order to enable a broader range of designs for coded aperture imaging systems. We provide a general framework and methods that generate richer and more flexible designs compared to the existing techniques. Besides this, we review and interpret the state-of-the-art uniformly redundant array designs, broaden the related concepts, and propose new design methods. © 2016 Optical Society of America

OCIS codes: (110.0110) Imaging systems; (170.1630) Coded aperture imaging; (340.7430) X-ray coded apertures; (110.3010) Image reconstruction techniques.

<http://dx.doi.org/10.1364/JOSAA.33.000863>

1. INTRODUCTION

Imaging using high-energy radiation with a spectrum ranging from x ray to γ ray has found many applications, including high-energy astronomy [1,2] and medical imaging [3–5]. In these wavelengths, imaging using lenses is not possible since the rays cannot be refracted or reflected, and hence cannot be focused. An alternative technique to do imaging in this spectrum is to use pinhole cameras, in which the lenses are replaced with a tiny pinhole. The problem in these cameras is that the pinholes pass a low intensity light, while for imaging purposes, a much stronger light is needed. Increasing the size of the pinhole cannot solve this problem as it increases the intensity at the expense of decreased resolution of the image. Coded aperture imaging (CAI) is introduced to address this issue by increasing the number of the pinholes. A coded aperture is a grating or grid that casts a coded image on a plane of detectors by blocking and unblocking the light in a known pattern, and produces a higher signal-to-noise ratio (SNR) of the image while maintaining a high angular resolution [6,7]. The coded image is then correlated with a decoding array in order to reconstruct the original image. The deployment of pinholes and the decoding array are usually jointly designed to make the reconstruction perfect or near-perfect. Figure 1 gives a schematic diagram of a CAI system. We emphasize that the theory's physical assumptions are: (1) each radiating point in the object produces an image with a constant magnification of the aperture; (2) the radiation is isotropic with respect to the detector area. Coded aperture designs for cases where (1) and (2) are violated have also been studied, for example in [8].

A coded aperture is usually defined based on an integer lattice, and can therefore be modeled as a two-dimensional array. For generality, we define the encoding array $C[c_1, c_2, \dots, c_n]$, $c_1, c_2, \dots, c_n \in \mathbb{Z}$, as an n -dimensional array with complex-valued entries and

$$C[c_1, \dots, c_n] = 0, \\ (c_1, \dots, c_n) \notin [0, L_1 - 1] \times \dots \times [0, L_n - 1].$$

For simplicity, $C[c_1, \dots, c_n]$ is also denoted by $C[\mathbf{a}]$, where $\mathbf{a} = [c_1, \dots, c_n]^T \in \mathbb{R}^n$. The decoding array D can be defined likewise. The set from which the elements of the aperture arrays take values from is referred to as an “alphabet.” In coded aperture imaging, a physically realizable coding aperture usually consists of binary alphabet, where 0 and 1 respectively represent closed and open pinholes. A complex-valued array C can be constructed by properly combining multiple coded images obtained from different aperture masks [9,10]. We show that the number of $\{0, 1\}$ masks needed to build an N -phase alphabet set is $(3N - 1)/2$ for odd N and N for even N . The calculations are based on the following facts: implementing a root of unity in the form of $x + iy$, $xy \neq 0$ ($i^2 = -1$) requires two masks, a pair in the form of $(x + iy, x - iy)$ or $(x + iy, -x + iy)$, $xy \neq 0$ requires three masks, and $1, -1, i, -i$ each requires one mask. In this work, we assume that the elements of an aperture could be unimodular complex numbers. In the future, the development in the hardware technology may make the implementation of the spatial phase modulators possible for γ ray, which can lead to realizable complex-valued physical masks. In that case, if both

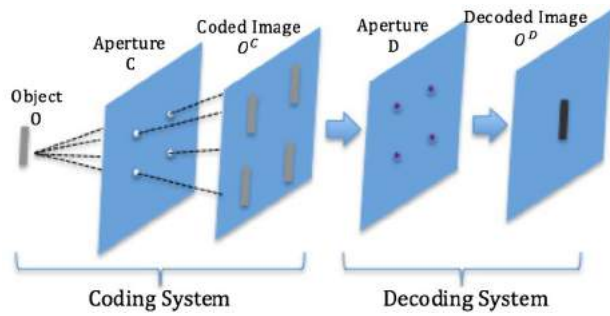


Fig. 1. Illustration of the CAI system.

coding and decoding systems use such masks, an analog reconstruction could be obtained.

For a planar object that is projected onto a gamma camera through a coding aperture, the object is perfectly decoded if $C * D = m\delta[\mathbf{r}]$, where $*$ denotes the convolution, m is an integer, $m \leq \omega$ with $\omega = L_1 L_2 \cdots L_n$ being the number of pinholes, and $\delta[\mathbf{r}]$ is the discrete delta function, which corresponds to an array with 1 centered at the origin and 0 elsewhere [3,7]. The value of m is also called “the SNR gain,” and larger m 's correspond to a better reconstruction quality.

The designs of the coded apertures are connected to the concept of “autocorrelation.” The autocorrelation can be defined in two different ways: periodic and aperiodic, and both of them can be used in the design of the coded apertures through different approaches, as will be pointed out later in this paper. The aperiodic autocorrelation function $A^C(\cdot)$ is defined as

$$A^C(v_1, \dots, v_n) = \sum_{c_1, \dots, c_n \in \mathbb{Z}} C[c_1, \dots, c_n] \overline{C[c_1 + v_1, \dots, c_n + v_n]}$$

where $v_1, v_2, \dots, v_n \in \mathbb{Z}$ and \bar{c} is the complex conjugate of c . The periodic autocorrelation will be defined later in the paper. By choosing $D = C^-$, where $C^-[c_1, \dots, c_n] = \overline{C[-c_1, \dots, -c_n]}$, $C * D$ gives the autocorrelation of C .

Nonredundant arrays (NRAs) have been introduced to arrange the pinholes in CAI, since they have the property that the aperiodic autocorrelations consist of a central spike with sidelobes equal to one within certain lag (range of the argument v_1, v_2, \dots, v_n) and either zero or unity beyond the lag [11]. Pseudonoise arrays (PNAs) [12] are another alternative, whose periodic autocorrelations consist of a central spike with -1 sidelobes, which lead to designs of a pair of arrays such that their convolution is a multiple of the discrete delta function [13]. Twin primes, quadratic residues, and m -sequences are examples of PNA designs. NRA- and PNA-based designs are both referred to as uniformly redundant arrays (URAs) [7,13,14]. However, the sizes of the URA structures are restricted and cannot be adapted to any particular detector [2,15]. Besides this, the SNR gain for URAs is limited to $\omega/2$ [7,16–18]. Other designs that have also been used in CAI are geometric design [19] and pseudonoise product design [20], but they are also available only for a limited number of sizes—the former design is for square arrays, and the latter one requires that pseudonoise sequences exist for each dimension.

Though it is generally hard to find a single pair of coding and decoding arrays, it might be easier to find several pairs that act perfectly while combined together. Based on this idea, we look for a broader range of designs for the coding arrays in this paper. We show that the aperture can be customized to any shape (boundary) on any lattice, satisfying various demands in practical situations. Our work is inspired by the Golay complementary arrays, which are defined as a pair of arrays whose aperiodic autocorrelations sum to zero in all out-of-phase positions. They have been used for pinhole arrangement in order to obtain the maximum achievable SNR gain, while eliminating the sidelobes of the decoded image [3]. We note that there is a natural mapping between a pair of Golay complementary arrays, say C_1 and C_2 , and a CAI system consisting of two parallel coding/decoding apertures, as illustrated in Fig. 2, where $D_1 = C_1^-$, $D_2 = C_2^-$. When an object goes through the system, the sidelobes are completely canceled out by adding the two decoded images.

Though an aperture is usually defined based on an integer lattice, we consider the design problem in the context of a general lattice, naturally arising from practical implementations. For example, usually the distance between two pinholes should be no less than a given threshold due to the physical constraints. It has been shown by Fejes [21] that the lattice arrangement of circles with the highest density in the two-dimensional Euclidean space is the hexagonal packing arrangement, in which the centers of the circles are arranged in a hexagonal lattice. Thus, given the minimal distance allowed among pinholes, the most compact arrangement (which corresponds to the largest possible SNR gain) is hexagonal lattice.

The outline of this paper is given below. In Section 2 we briefly present related work on Golay complementary array pairs which are based on aperiodic autocorrelation, and then propose complementary lattice arrays and other related new concepts, such as the complementary array banks. This general framework leads to the new concept called multichannel CAI systems, which extends the classical CAI systems. We provide the concept, theory, and the design methodology. Due to the reasons mentioned before, our examples are mainly based on two-dimensional hexagonal arrays and unimodular alphabets, which consist of unimodular complex numbers. Nevertheless, the methodology given in this work could be further generalized to higher dimensions. In Section 3 we review the URA literature that is mostly based on periodic autocorrelation. We further generalize the related concepts in Section 4 in a similar fashion. This leads to a new class of aperture designs that exist for sizes for which URAs do not, while having the desirable imaging characteristics of URAs. In Section 5, we provide computer simulations demonstrating the performance of our schemes.

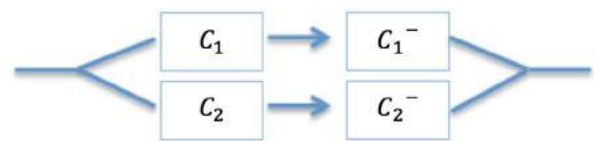


Fig. 2. CAI system with two parallel channels: a planar object is the input to the coding apertures C_1 , C_2 , and a decoded image is the output from the decoding apertures C_1^- , C_2^- .

2. CONCEPT, THEORY, AND DESIGN OF COMPLEMENTARY LATTICE ARRAYS

A. Golay Complementary Arrays

In this section we briefly introduce related works on Golay complementary array pairs. Golay [22] first introduced Golay complementary sequence pairs in 1951 to address the optical problem of multislit spectrometry. These sequences were later used for many other applications, including horizontal modulation systems in communication [23], orthogonal frequency division multiplexing [24], Ising spin systems [25], and channel measurement [26,27]. Barker arrays, which are closely related to complementary array pairs [28], are a $\{\pm 1\}$ binary array C such that for all $v_1, \dots, v_n \in \mathbb{Z}, (v_1, \dots, v_n) \neq (0, \dots, 0)$,

$$|A^C(v_1, \dots, v_n)| \leq 1. \tag{1}$$

Another related concept is the NRA, which also satisfies the condition (1). Its only difference with the Barker array is that it is $\{0, 1\}$ -binary.

Golay complementary array pairs address the scarcity of Barker arrays and NRAs. The basic idea of Golay complementary array pairs is to use the nonzero part of one autocorrelation to “compensate” the nonzero counterpart of the other [22]. Specifically, a pair of arrays C_1 and C_2 of size $L_1 \times \dots \times L_n$ is a Golay complementary array pair, if the sum of their aperiodic autocorrelations is a multiple of the discrete delta function, i.e.,

$$A^{C_1}(v_1, \dots, v_n) + A^{C_2}(v_1, \dots, v_n) = 0,$$

for all $v_1, \dots, v_n \in \mathbb{Z}, (v_1, \dots, v_n) \neq (0, \dots, 0)$. The initial study of Golay complementary sequence pairs ($n = 1$) was for the binary case. Binary Golay complementary sequence pairs are known for lengths 2, 10 [23], and 26 [29]. It has been shown that infinitely many lengths could be synthesized using the existing solutions [30]. Specifically, binary Golay complementary sequence pairs with length $2^{k_1} 10^{k_2} 26^{k_3}$ exist, where k_1, k_2, k_3 are any nonnegative integers. Besides, no sequences of other lengths have been found. Later on, larger alphabets were considered, including 2^n -phase [31], N -phase for even N [32], the ternary case $\mathfrak{A} = \{-1, 0, 1\}$ [33–35], and the unimodular case [36]. Here, an alphabet \mathfrak{A} is called N -phase if it consists of N th roots of unity, i.e., $\mathfrak{A} = \{\zeta : \zeta^N = 1\}$; it is unimodular if $\mathfrak{A} = \{\zeta : |\zeta| = 1\}$.

In 1978, Ohyama *et al.* [3] constructed binary Golay complementary array pairs ($n = 2$) of size $2^{k_1} \times 2^{k_2}$. The size is then generalized to $2^{k_1} 10^{k_2} 26^{k_3} \times 2^{k_4} 10^{k_5} 26^{k_6}$, where k_j 's, $j = 1, \dots, 6$ are any nonnegative integers [37,38].

We look for broader concepts and designs than complementary array pairs. The examples provided in this paper are for the two-dimensional case, but they can be easily generalized to higher dimensions. We start with the definitions in the following subsection.

B. Definitions and Notations

Definition 1 A *lattice* in \mathbb{R}^n is a subgroup of \mathbb{R}^n , which is generated from a basis by forming all linear combinations with integer coefficients. In other words, a lattice \mathfrak{L} in \mathbb{R}^n has the form

$$\mathfrak{L} = \left\{ \sum_{i=1}^n c_i \mathbf{e}_i \mid c_i \in \mathbb{Z} \right\},$$

where $\{\mathbf{e}_i\}_{i=1}^n$ forms a basis of \mathbb{R}^n .

For example, the integer lattice \mathbb{Z}^2 is generated from the basis $\mathbf{e}_1 = (1, 0)$, $\mathbf{e}_2 = (0, 1)$. The hexagonal (honeycomb) lattice \mathbb{A}_2 is generated from the basis $\mathbf{e}_1 = (1, 0)$, $\mathbf{e}_2 = (-\frac{1}{2}, \frac{\sqrt{3}}{2})$. A classical array is based on an integer lattice. We now give the definition of an array that is based on a general lattice.

Definition 2 Let \mathfrak{L} be a lattice. A *lattice array* $C^{\mathfrak{L}, \Omega, \mathfrak{A}}$ defined over alphabet \mathfrak{A} and with support Ω is a mapping $C[\cdot]: \mathfrak{L} \rightarrow \mathfrak{A}$, such that $C[\mathbf{a}] = 0$ for all $\mathbf{a} \notin \Omega$ and $C[\mathbf{a}] \in \mathfrak{A}$ for all $\mathbf{a} \in \Omega$, where $C[\mathbf{a}]$ is the entry at location \mathbf{a} . The number of the elements of Ω (array size) is denoted by $|\Omega|$. We denote $C^{\mathfrak{L}, \Omega, \mathfrak{A}}$ by C when there is no ambiguity.

The following terms are made to simplify the notations.

- Define $C^{\mathfrak{L}, \Omega + \mathbf{t}, \mathfrak{A}}\{\mathbf{t}\}$ as the **shifted copy** of $C^{\mathfrak{L}, \Omega, \mathfrak{A}}$ by \mathbf{t} (for $\mathbf{t} \in \mathfrak{L}$), if

$$C^{\mathfrak{L}, \Omega + \mathbf{t}, \mathfrak{A}}\{\mathbf{t}\}[\mathbf{a}] = C^{\mathfrak{L}, \Omega, \mathfrak{A}}[\mathbf{a} - \mathbf{t}], \quad \forall \mathbf{a} \in \mathfrak{L}.$$

For brevity, $C^{\mathfrak{L}, \Omega + \mathbf{t}, \mathfrak{A}}\{\mathbf{t}\}$ is simplified as $C\{\mathbf{t}\}$.

- Assume that the two arrays $C_1^{\mathfrak{L}, \Omega_1, \mathfrak{A}_1}$ and $C_2^{\mathfrak{L}, \Omega_2, \mathfrak{A}_2}$ are based on the same lattice \mathfrak{L} , but not necessarily on the same area. The **addition** of C_1 and C_2 , $C = C_1 + C_2$, is an array whose entries are the addition of corresponding entries in C_1 and C_2 , i.e.,

$$\Omega = \Omega_1 \cup \Omega_2, \quad C[\mathbf{a}] = C_1[\mathbf{a}] + C_2[\mathbf{a}], \quad \forall \mathbf{a} \in \Omega.$$

- A set of arrays $\{C_m^{\mathfrak{L}, \Omega_m, \mathfrak{A}_m}\}_{m=1}^M$ are **nonoverlapping** if $\Omega_{m_1} \cap \Omega_{m_2} = \emptyset, \quad \forall m_1, m_2 \in 1, 2, \dots, M, m_1 \neq m_2.$

Definition 3 Assume that the lattice \mathfrak{L} is generated from $\{\mathbf{e}_i\}_{i=1}^n$. The **aperiodic autocorrelation** function is

$$A^C(v_1, \dots, v_n) = \sum_{\mathbf{a} \in \Omega} C[\mathbf{a}] \overline{C[\mathbf{a} + v_1 \mathbf{e}_1 + \dots + v_n \mathbf{e}_n]},$$

for $v_1, v_2, \dots, v_n \in \mathbb{Z}$. The **aperiodic cross-correlation** function $A^{C_1 C_2}(\cdot)$ of two arrays C_1 and C_2 is

$$A^{C_1 C_2}(v_1, \dots, v_n) = \sum_{\mathbf{a} \in \Omega} C_1[\mathbf{a}] \overline{C_2[\mathbf{a} + v_1 \mathbf{e}_1 + \dots + v_n \mathbf{e}_n]}.$$

Sometimes, $A^C(\cdot)$ and $A^{C_1 C_2}(\cdot)$ are respectively denoted by C^+ and $C_1 * C_2^-$.

Definition 4 A **complementary array bank** consists of pairs $\{(C_m^{\mathfrak{L}, \Omega_{1m}, \mathfrak{A}_1}, D_m^{\mathfrak{L}, \Omega_{2m}, \mathfrak{A}_2})\}_{m=1}^M$ such that the sum of the cross-correlations is a multiple of the discrete delta function,

$$\sum_{m=1}^M C_m * D_m^- = \sum_{m=1}^M A^{C_m D_m^-}(\cdot) = \omega \delta[\mathbf{r}],$$

where ω is a constant. M is called the *order*, or *number of channels*.

Remark 1 There is a natural mapping between a complementary array bank, say $\{(C_m, D_m)\}_{m=1}^M$, and a CAI system consisting of M parallel channels, each of which consists of a pair of coding and decoding apertures (Fig. 3). When a source image comes, it is coded and decoded through M channels simultaneously, and is then retrieved by simply adding the decoded images from all the channels. The multichannel CAI system proposed here provides a

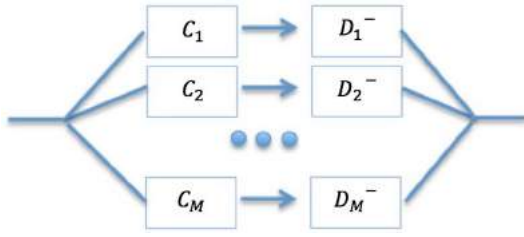


Fig. 3. CAI system with M parallel channels: a planar object is the input to the coding apertures C_1, \dots, C_M , and a decoded image is the output from the decoding apertures D_1^-, \dots, D_M^- .

generalized solution to CAI design, by including a classical CAI system as a special case. In the remaining part of Section 2, we mainly study the complementary array sets, which provides insight into the theory and design of complementary array banks in general.

Definition 5 A set of arrays $\{C_m^{\mathcal{L}, \Omega, \mathfrak{A}}\}_{m=1}^M$ is a **complementary array set** if the sum of their aperiodic autocorrelations is a multiple of the discrete delta function, i.e.,

$$\sum_{m=1}^M A^{C_m}(v_1, v_2, \dots, v_n) = 0, \quad (2)$$

for all $v_1, v_2, \dots, v_n \in \mathbb{Z}$, $(v_1, \dots, v_n) \neq (0, \dots, 0)$. A Golay complementary array pair is the special case when $M = 2$.

Remark 2 In practice, the pinholes on an aperture only change the phase of a source point. Therefore, we assume a unimodular alphabet by default. It is clear that if a set of nonoverlapping arrays are based on unimodular/ N -phase alphabets, the addition of them is also based on an unimodular/ N -phase alphabet.

The autocorrelation of any array is the same as that of its shifted copy. This is because for any $v_1, \dots, v_n \in \mathbb{Z}$, $\mathbf{t} \in \mathcal{L}$, we have

$$\begin{aligned} A^{C\{\mathbf{t}\}}(v_1, \dots, v_n) &= \sum_{\mathbf{a} \in \Omega + \mathbf{t}} C\{\mathbf{t}\}[\mathbf{a}] \overline{C\{\mathbf{t}\}[\mathbf{a} + v_1 \mathbf{e}_1 + \dots + v_n \mathbf{e}_n]} \\ &= \sum_{\mathbf{a} \in \Omega + \mathbf{t}} C[\mathbf{a} - \mathbf{t}] \overline{C[\mathbf{a} - \mathbf{t} + v_1 \mathbf{e}_1 + \dots + v_n \mathbf{e}_n]} \\ &= \sum_{\mathbf{a} \in \Omega} C[\mathbf{a}] \overline{C[\mathbf{a} + v_1 \mathbf{e}_1 + \dots + v_n \mathbf{e}_n]} \\ &= A^C(v_1, \dots, v_n). \end{aligned}$$

Furthermore, if $\{C_m\}_{m=1}^M$ is a complementary array set, then $\{C_m\{\mathbf{t}_m\}\}_{m=1}^M$, $\forall \mathbf{t}_m \in \mathcal{L}$ also forms a complementary array set. In other words, a complementary array set is “invariant” under shift operation.

Based on a unimodular alphabet, a complementary array set $\{C_m\}_{m=1}^M$ satisfies $\sum_{m=1}^M A^{C_m}(0, \dots, 0) = M|\Omega|$. Thus, the sum of the autocorrelations can be written as a multiple of the discrete delta function: $\sum_{m=1}^M C_m * C_m = \sum_{m=1}^M A^{C_m}(\cdot) = M|\Omega|\delta[\mathbf{r}]$.

C. Motivating Design

In Ohyama *et al.*'s design, \mathcal{L} is an integer lattice, and the number of complementary arrays is $M = 2$. The design consists of two steps:

- First, choose the following complementary sequence pair:

$$C_1 = [1 \ 1], \quad C_2 = [1 \ -1]. \quad (3)$$

- Second, design complementary array pairs of larger sizes in an inductive manner. Assume that we already have a complementary pair C_1, C_2 , with $C_1 * C_1^- + C_2 * C_2^- = 2\omega\delta[\mathbf{r}]$, where ω is constant. Let

$$\hat{C}_1 = C_1\{\mathbf{t}_1\} + C_2\{\mathbf{t}_2\}, \quad \hat{C}_2 = C_1\{\mathbf{t}_1\} - C_2\{\mathbf{t}_2\}, \quad (4)$$

where the shifts \mathbf{t}_1 and \mathbf{t}_2 are arbitrarily chosen.

The validity of the construction Eq. (4) is clear from the fact that

$$\begin{aligned} \hat{C}_1 * \hat{C}_1^- &= C_1\{\mathbf{t}_1\} * C_1\{\mathbf{t}_1\}^- + C_2\{\mathbf{t}_2\} * C_2\{\mathbf{t}_2\}^- \\ &\quad + C_1\{\mathbf{t}_1\} * C_2\{\mathbf{t}_2\}^- + C_2\{\mathbf{t}_2\} * C_1\{\mathbf{t}_1\}^-, \\ \hat{C}_2 * \hat{C}_2^- &= C_1\{\mathbf{t}_1\} * C_1\{\mathbf{t}_1\}^- + C_2\{\mathbf{t}_2\} * C_2\{\mathbf{t}_2\}^- \\ &\quad - C_1\{\mathbf{t}_1\} * C_2\{\mathbf{t}_2\}^- - C_2\{\mathbf{t}_2\} * C_1\{\mathbf{t}_1\}^-, \end{aligned}$$

and thus,

$$\begin{aligned} \hat{C}_1 * \hat{C}_1^- + \hat{C}_2 * \hat{C}_2^- &= 2(C_1\{\mathbf{t}_1\} * C_1\{\mathbf{t}_1\}^- + C_2\{\mathbf{t}_2\} * C_2\{\mathbf{t}_2\}^-) \\ &= 2(C_1 * C_1^- + C_2 * C_2^-) = 4\omega\delta[\mathbf{r}]. \end{aligned} \quad (5)$$

In practice, \mathbf{t}_1 and \mathbf{t}_2 are chosen properly so that $C_1\{\mathbf{t}_1\}$ and $C_2\{\mathbf{t}_2\}$ do not overlap, which guarantees that \hat{C}_1 and \hat{C}_2 are still based on unimodular alphabets. For example, after applying Eqs. (4) to Eq. (3) once, we have two possible complementary array pairs:

$$\hat{C}_1 = [1 \ 1 \ 1 \ -1], \quad \hat{C}_2 = [1 \ 1 \ -1 \ 1]; \quad (6)$$

or

$$\hat{C}_1 = \begin{bmatrix} 1 & 1 \\ 1 & -1 \end{bmatrix}, \quad \hat{C}_2 = \begin{bmatrix} 1 & 1 \\ -1 & 1 \end{bmatrix}. \quad (7)$$

The process of design is also illustrated in Fig. 4. By repeated applications of the above design process, complementary pairs of size $2^{k_1} \times 2^{k_2}$ (for any nonnegative integers k_1, k_2) can be designed.

Inspired by the above design for complementary array pairs on integer lattices, we look for a “seed” [similar to Eq. (3)] and a related scheme to “grow” the seed [similar to Eq. (4)] for the design of complementary hexagonal arrays. Admittedly, we build a simple mapping between two-dimensional arrays on an integer lattice and a hexagonal lattice (or other lattices) below:

$$C^{\mathcal{L}, \Omega, \mathfrak{A}}[c_1 * \mathbf{e}_1^i + c_2 * \mathbf{e}_2^j] = C^{\mathcal{L}^h, \Omega^h, \mathfrak{A}}[c_1 * \mathbf{e}_1^h + c_2 * \mathbf{e}_2^h], \quad (8)$$

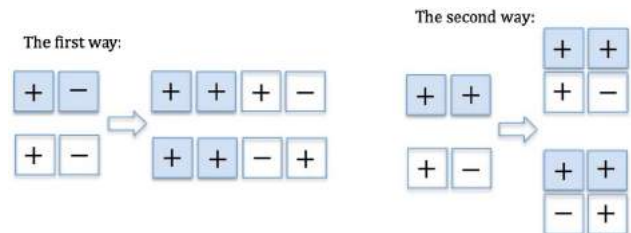


Fig. 4. Illustration of the design of complementary array pairs on integer lattices.

for all $c_1, c_2 \in \mathbb{Z}$, where the superscripts s and h respectively denote integer and hexagonal lattices. Under the above mapping, a set of complementary arrays on an integer lattice are still complementary on a hexagonal lattice. This is due to the fact that the autocorrelation of an array is only with respect to the coefficients c_1, c_2 . Nevertheless, the lattice array naturally arises from practical designs. Consider the scenario where a two- (or three)-dimensional coded aperture is to be built that has pinholes arranged on a certain (suitably chosen) type of lattice, which adapts to a particular physical aperture mask. The designs are preferably based on that particular lattice instead of its mapping on an integer lattice, which has zero elements padded here and there and which needs to be mapped back to the original lattice.

D. Design for the Basic Hexagonal Array of Seven Points

We first study a very simple hexagonal pattern that acts as a “seed.” It is a hexagonal array of seven points, which is shown in Fig. 5. After that, we consider possible ways to “grow” the seed.

We start from considering the existence of hexagonal complementary array pairs, i.e., the order M is 2.

Theorem 1 For the basic seven-point hexagonal array, there exists no complementary array pair with a unimodular alphabet (Fig. 6).

The proof is given in Appendix A. One may be further interested in the existence of a hexagonal complementary array pair if the basic array does not have the origin 0 (Fig. 7). In fact, it does not exist, either.

Theorem 2 For the array in Fig. 7, there exists no hexagonal complementary array pair with a unimodular alphabet.

The proof is given in Appendix B. The nonexistence of complementary array pairs for the array in Fig. 5 motivates us to further consider higher-order M . We use the notation



Fig. 5. Basic hexagonal array with seven points.

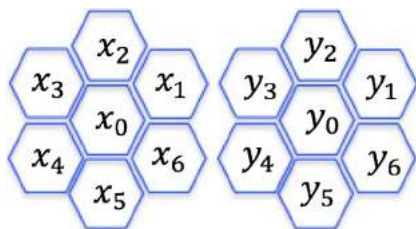


Fig. 6. There exists no seven-point hexagonal complementary pair with unimodular alphabet.

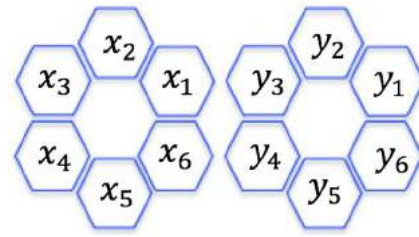


Fig. 7. Basic hexagonal array with six points.

of “design parameter” for brevity. For a particular array pattern, if there is a complementary array set with M arrays and an N -phase alphabet, the pair (M, N) is called its **design parameters**. Furthermore, if the size of each array is equal to L , we refer to the triplet (M, N, L) as its **design parameters** whenever there is no ambiguity.

Fortunately, complementary array triplets with an unimodular alphabet exist. In fact, we have found more than one design with $(M, N, L) = (3, 3, 7)$. The following is an example.

Design 1 Let $\zeta = \exp(i2\pi/3)$. Let

$$C_1 = \{x_k\}_{k=0}^6, \quad C_2 = \{y_k\}_{k=0}^6, \quad C_3 = \{z_k\}_{k=0}^6$$

denote the entries of three hexagonal arrays shown in Fig. 5. Then

$$\begin{aligned} \{x_k\}_{k=0}^6 &= \{\zeta^2, \zeta^0, \zeta^2, \zeta^2, \zeta^0, \zeta^2, \zeta^0\}, \\ \{y_k\}_{k=0}^6 &= \{\zeta^1, \zeta^0, \zeta^2, \zeta^2, \zeta^1, \zeta^0, \zeta^1\}, \\ \{z_k\}_{k=0}^6 &= \{\zeta^1, \zeta^0, \zeta^1, \zeta^1, \zeta^2, \zeta^0, \zeta^1\} \end{aligned}$$

form a complementary array set (Fig. 8).

We have also found more than one design with $(M, N, L) = (4, 2, 7)$. The following is an example.

Design 2 Let

$$\begin{aligned} C_1 &= \{x_k\}_{k=0}^6, \quad C_2 = \{y_k\}_{k=0}^6, \\ C_3 &= \{z_k\}_{k=0}^6, \quad C_4 = \{w_k\}_{k=0}^6 \end{aligned}$$

denote the entries of four hexagonal arrays shown in Fig. 5. Then

$$\begin{aligned} \{x_k\}_{k=0}^6 &= \{1, 1, -1, 1, 1, -1, 1\}, \\ \{y_k\}_{k=0}^6 &= \{-1, 1, 1, -1, -1, 1, 1\}, \\ \{z_k\}_{k=0}^6 &= \{1, 1, -1, 1, -1, 1, 1\}, \\ \{w_k\}_{k=0}^6 &= \{1, 1, 1, -1, 1, -1, 1\} \end{aligned}$$

form a complementary array set (Fig. 9).

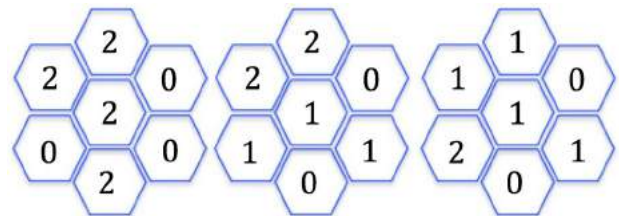


Fig. 8. Complementary triplet with three-phase alphabet, i.e., $(M, N, L) = (3, 3, 7)$, where ζ^k is represented by k , for $k = 0, 1, 2$.

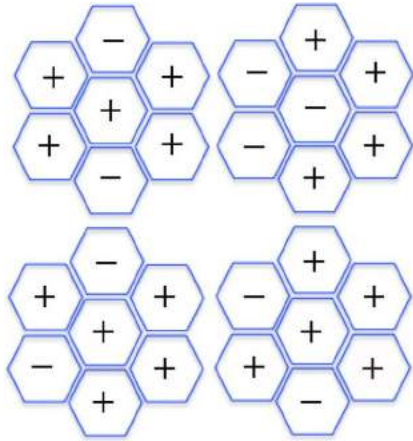


Fig. 9. Complementary quadruplet with two-phase (binary) alphabet, i.e., $(M, N, L) = (4, 2, 7)$, where ± 1 is represented by \pm .

E. Methodology for Designing Larger Arrays

We now consider how to “grow” the seed that we have found in order to design more and larger arrays. If $+$ and $*$ are respectively considered as addition and multiplication operations, then Eqs. (4) and (5) can be written in symbolic expression,

$$\hat{C} = \mathbf{H}\mathbf{C}\{\mathbf{t}\}, \quad (9)$$

$$\hat{C}^T \hat{C}^- = \mathbf{C}\{\mathbf{t}\}^T \mathbf{H}^T \mathbf{H} \mathbf{C}\{\mathbf{t}\}^- = 2\mathbf{C}\{\mathbf{t}\}^T \mathbf{C}\{\mathbf{t}\}^-, \quad (10)$$

where

$$\hat{C} = \begin{bmatrix} \hat{C}_1 \\ \hat{C}_2 \end{bmatrix}, \quad \hat{C}^- = \begin{bmatrix} \hat{C}_1^- \\ \hat{C}_2^- \end{bmatrix},$$

$$\mathbf{H} = \begin{bmatrix} 1 & 1 \\ 1 & -1 \end{bmatrix}, \quad \mathbf{C}\{\mathbf{t}\} = \begin{bmatrix} C_1\{\mathbf{t}_1\} \\ C_2\{\mathbf{t}_2\} \end{bmatrix},$$

and \mathbf{H}^T is the conjugate transpose of \mathbf{H} . The key that \hat{C} remains to be a complementary pair is that \mathbf{H} satisfies $\mathbf{H}^T \mathbf{H} = 2\mathbf{I}$, i.e., \mathbf{H} is a Hadamard matrix. This observation could be generalized to the following result.

Theorem 3 Let $\mathbf{U} = [u_{mk}]_{M \times M}$ be a unitary matrix up to a constant, i.e., $\mathbf{U}^T \mathbf{U} = c\mathbf{I}$, where $c > 0$. Assume that $\{C_k^{\xi, \Omega_k, \mathfrak{A}}\}_{k=1}^M$ is a complementary array set. Then, $\{\hat{C}_m\}_{m=1}^M$ is also a complementary array set, where

$$\hat{C}_m = \sum_{k=1}^M u_{mk} \cdot C_k^{\xi, \Omega_k + \mathbf{t}_k, \mathfrak{A}}\{\mathbf{t}_k\}, \quad m = 1, 2, \dots, M,$$

$\mathbf{t}_1, \mathbf{t}_2, \dots, \mathbf{t}_M$ are arbitrarily chosen, and $u \cdot C$ is an array that multiplies each entry of C by the scalar u .

Proof 1 Define a vector space on \mathfrak{A} (it is not necessarily a field) with the addition operation $+$ defined in Definition 2, and the variables

$$\hat{C} = \begin{bmatrix} \hat{C}_1 \\ \vdots \\ \hat{C}_M \end{bmatrix} \quad \text{and} \quad \mathbf{C}\{\mathbf{t}\} = \begin{bmatrix} C_1\{\mathbf{t}_1\} \\ \vdots \\ C_M\{\mathbf{t}_M\} \end{bmatrix}.$$

Define a quadratic form with the multiplication operation $*$ defined as the convolution. The sum of aperiodic autocorrelations of $\{\hat{C}_m\}_{m=1}^M$ is

$$\begin{aligned} \sum_{m=1}^M \hat{C}_m * \hat{C}_m^- &= \hat{C}^T \hat{C}^- = \mathbf{C}\{\mathbf{t}\}^T \mathbf{U}^T \mathbf{U} \mathbf{C}\{\mathbf{t}\}^- = c\mathbf{C}\{\mathbf{t}\}^T \mathbf{C}\{\mathbf{t}\}^- \\ &= c \sum_{m=1}^M C_m\{\mathbf{t}_M\} * C_m\{\mathbf{t}_M\}^- \\ &= c \sum_{m=1}^M C_m * C_m^- = cM\omega\delta[\mathbf{r}]. \end{aligned} \quad (11)$$

Remark 3 We are interested in the following special case where

1. \mathfrak{A} is an N -phase alphabet;
2. \mathbf{U} is the Fourier matrix: $\mathbf{F}_M = [f_{mk}]_{M \times M}$, $f_{mk} = \exp\{i2\pi(m-1)(k-1)/M\}$;
3. The shifted arrays $C_k^{\xi, \Omega_k + \mathbf{t}_k, \mathfrak{A}}\{\mathbf{t}_k\}$, $k = 1, \dots, M$ do not overlap. The complementary array set $\{C_k\}_{k=1}^M$ with design parameters $(M, N, |\Omega|)$ (if $|\Omega_k| = |\Omega|$, $k = 1, \dots, M$) becomes $\{\hat{C}_m\}_{m=1}^M$ with design parameters $(M, \text{lcm}(N, M), M|\Omega|)$ according to Theorem 3, where lcm stands for least common multiple. Besides this, we have $c = M$, $\omega = |\Omega|$ in Eq. (11).

Theorem 3 provides a powerful tool to design more complex complementary arrays, which will be illustrated in Subsection 2.F. For future reference, we also include the following fact.

Remark 4 Assume that $\mathbf{C}^{(1)}, \dots, \mathbf{C}^{(K)}$ are K complementary array sets on the same lattice, and the set $\mathbf{C}^{(k)}$ has design parameters (M_k, N_k) , $\forall k = 1, \dots, K$. Then, it is clear that $\mathbf{C} = \mathbf{C}^{(1)} \cup \dots \cup \mathbf{C}^{(K)}$ can be thought as a new complementary set with design parameters $(\sum_{k=1}^K M_k, \text{lcm}(N_1, \dots, N_K))$.

F. Example: Design for the Hexagonal Array of 18 Points

The basic hexagonal array of seven points studied in Subsection 2.D contains two layers, with one and six points, respectively. We now study the hexagonal array that contains one more layer (shown in Fig. 10). The design for this hexagonal array is not very obvious, so we delete the center element, i.e., layer 1. (In fact, designs always exist for an arbitrarily shaped array, as will be discussed later. We delete the center point primarily for a cute solution.) The remaining 18 points are grouped into six basic triangular arrays: $C_1, C_2, C_3, C'_1, C'_2, C'_3$, which is shown in Fig. 11.

This motivates the design of complementary array triplets for the basic triangular array shown in Fig. 12, where ζ^k is represented by k , for $k = 0, 1, 2$, $\zeta = \exp(i2\pi/3)$. In Fig. 12,

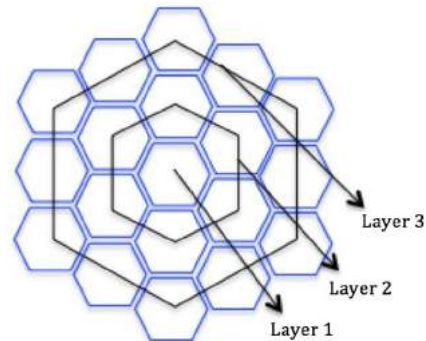


Fig. 10. Hexagonal array with three layers (19 points).

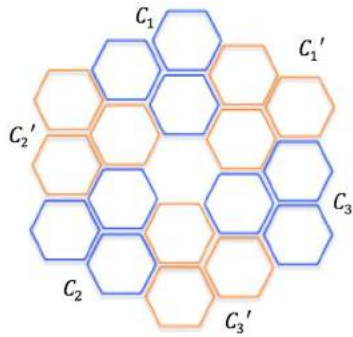


Fig. 11. Hexagonal array with layer 2 and 3 (18 points).

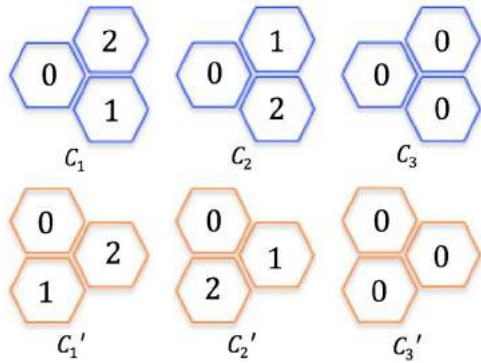


Fig. 12. Basic triangular complementary array triplets with three-phase alphabet, i.e., $(M, N, L) = (3, 3, 3)$.

$\{C_1, C_2, C_3\}$ form a complementary array set. Due to symmetry, its rotated copy, C'_1, C'_2, C'_3 , also forms a complementary array set. Applying Theorem 3, we obtain the following design.

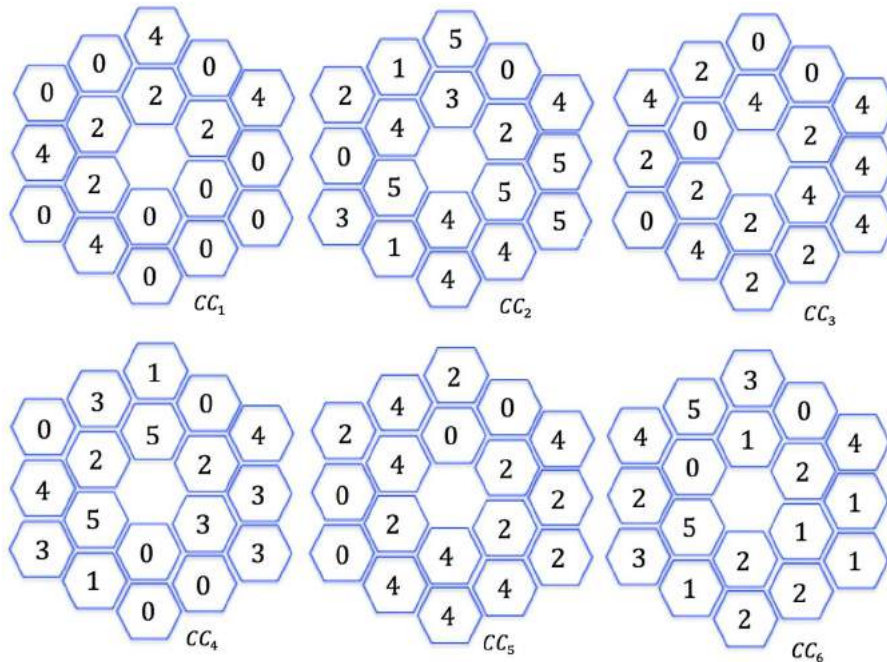


Fig. 13. Complementary array set with parameter $(M, N, L) = (6, 6, 18)$.

Design 3 Let

$$\hat{C} = \begin{bmatrix} \hat{C}_1 \\ \hat{C}_2 \\ \hat{C}_3 \\ \hat{C}_4 \\ \hat{C}_5 \\ \hat{C}_6 \end{bmatrix} = F_6 \begin{bmatrix} C'_1\{\mathbf{t}_1\} \\ C_1\{\mathbf{t}_2\} \\ C'_2\{\mathbf{t}_3\} \\ C_2\{\mathbf{t}_4\} \\ C'_3\{\mathbf{t}_5\} \\ C_3\{\mathbf{t}_6\} \end{bmatrix},$$

where $\mathbf{t}_1, \dots, \mathbf{t}_6$ are such that $\hat{C}_1, \dots, \hat{C}_6$ are arranged to form a hexagonal array of 18 points, as is shown in Fig. 11. Then $\{\hat{C}_m\}_{m=1}^6$ forms a complementary array set. The design is also shown in Fig. 13, where ζ^k is represented by k , for $k = 0, \dots, 5$, $\zeta = \exp(i2\pi/6)$.

G. Complementary Array Bank

Up to this point, we have assumed that the coding array C and decoding array D are related via $D[\mathbf{r}] = C[-\mathbf{r}]$. The design of CAI thus reduces to the design of complementary array sets. Then we extend the autocorrelation to cross-correlation, and the design of complementary array sets is accordingly extended to that of complementary array banks. The following result is a generalization of Theorem 3, and its proof is similar to that of Theorem 3.

Theorem 4 Let $\Theta = [\theta_{mk}]$, $\Phi = [\phi_{mk}] \in \mathbb{C}^{\tilde{M} \times M}$ be two matrices satisfying $\Theta^T \Phi = c\mathbf{I}$ for some positive constant c . For a given lattice \mathcal{L} , suppose that $\{(C_k, D_k)\}_{k=1}^M$ is a complementary array bank. Then, $\{(\hat{C}_m, \hat{D}_m)\}_{m=1}^{\tilde{M}}$ is also a complementary array bank, where

$$\hat{C}_m = \sum_{k=1}^M \theta_{mk} \cdot C_k\{\mathbf{t}_k\}, \hat{D}_m = \sum_{k=1}^M \phi_{mk} \cdot D_k\{\mathbf{t}_k\},$$

$$m = 1, \dots, \tilde{M},$$

t_1, t_2, \dots, t_M are arbitrarily chosen, and $u \cdot C$ is an array that multiplies each entry of C by the scalar u .

Remark 5 The following case is of interest.

1. $\{C_k, D_k\}_{k=1}^M$ have N -phase alphabets;
2. Θ is equal to Φ and it contains M orthogonal columns of the complex Fourier matrix $F_{\tilde{M}}$ (thus $M \leq \tilde{M}$);
3. The shifted arrays $C_k\{t_k\}$ do not overlap, neither do $D_k\{t_k\}$, $k = 1, \dots, M$.

Furthermore, if we assume that $C_k = D_k$, $k = 1, \dots, M$ and the array sizes are equal to L , then the complementary array set $\{C_k\}_{k=1}^M$ has design parameters (M, N, L) , and $\{\hat{C}_m\}_{m=1}^M$ has design parameters $(\tilde{M}, \text{lcm}(N, \tilde{M}), ML)$.

Lemma 1 Any single point, as the simplest array on any lattice, forms a complementary set.

Remark 6 Lemma 1 is a trivial but useful result. It follows from Definition 5 and the fact that the aperiodic autocorrelation of a single point is always the discrete delta function. By employing Lemma 1, Theorem 3, and Theorem 4, it is possible to design complementary arrays of various support Ω .

Corollary 1 For an arbitrary set Ω on a lattice, there exists at least one complementary array set with support Ω for any order M such that $M \geq |\Omega|$.

Remark 7 [Augmentation using Theorem 4] Due to Theorem 4, we let $\tilde{M} > M$ for practical purposes. For example, we choose $\tilde{M} = 2^m$ (for a positive integer m) such that \mathbf{U} is a ± 1 Hadamard matrix and the growth of alphabet (N) could be well controlled. We call this “augmentation” procedure. Augmentation is important, because it is often desirable to reduce the size of the alphabet, and thus the cost of practical implementations. The following design is an example of augmentation.

Design 4 We use several basic arrays to compose a smile face shown in Fig. 14. The colors indicate different basic complementary array sets: the two green arrays (at the lower and upper boundaries) form a basic array set with parameters $(M, N, L) = (2, 2, 8)$. So do the brown ones (at the lower-left and upper-right boundaries) and cyan ones (at the lower-right and upper-left boundaries). The two blue arrays (at the lower and upper boundaries) form a basic array set with $(M, N, L) = (2, 2, 4)$. The two yellow arrays (single points at the lower and upper boundaries) form a basic array set with $(M, N, L) = (2, 1, 1)$. The three black arrays (the eyes and nose) form a basic array set with $(M, N, L) = (3, 3, 3)$ (Fig. 12); so do the three red ones (part of the mouth).



Fig. 14. Smile design, with $(M, N, L) = (20, 60, 88)$ (without augmentation) or $(32, 6, 88)$ (with augmentation).

The four purple arrays (the rest part of the mouth) form a basic array set with parameters $(M, N, L) = (4, 2, 3)$, which could be obtained by applying Theorem 4 with Remark 5 and $\tilde{M} = 4$ to a set of three single-point arrays. By applying Remark 4 and Theorem 3 to the 20 arrays, a smile design with $(M, N, L) = (20, 60, 88)$ could be obtained. Due to Remark 7, another smile design with $(M, N, L) = (32, 6, 88)$ could be obtained.

H. Design for Infinitely Large Hexagonal Arrays

By choosing a proper seed and growth scheme, we are able to design infinitely large hexagonal arrays. The following is an example. We first design a complementary array set with $M = 7$, as a seed.

Design 5 The union of Design 1 with design parameters $(M, N, L) = (4, 2, 7)$ and Design 2 with $(M, N, L) = (3, 3, 7)$ is a design with $(M, N, L) = (4 + 3, \text{lcm}(2, 3), 7) = (7, 6, 7)$ (Fig. 5), based on Remark 4.

Design 6 By repeated applications of Theorem 3 with $\mathbf{U} = \mathbf{F}_7$ to Design 5, we obtain a design with parameters $(M, N, L) = (7, 42, 7^\ell)$ for any positive integer ℓ . The design is illustrated in Fig. 15, where the colors indicate the process of “growth.” In fact, applying Theorem 3 to Design 5 once (with Remark 3 conditions), we obtain a larger array set with $(M, N, L) = (7, \text{lcm}(6, 7), 7 \times 7) = (7, 42, 7^2)$. Figure 15(a) illustrates how the seven arrays of size 7 (indicated by different colors) are combined to form larger arrays. Similarly, applying Theorem 3 to the $(M, N, L) = (7, 42, 7^2)$ design once, we obtain a larger array set with $(M, N, L) = (7, \text{lcm}(42, 7), 7 \times 7^2) = (7, 42, 7^3)$. Figure 15(b) illustrates how the seven arrays of size 7^2 (indicated by different colors) are combined to form larger arrays. Further applications of Theorem 3 will not increase M, N , but will increase L .

As an alternative, the following design is also for a 7^ℓ -point hexagonal array, but with different elements.

Design 7 We keep applying Theorem 3 with $\mathbf{U} = \mathbf{F}_7$ to a single-point array, e.g., with entry 1, we obtain a design with parameters $(M, N, L) = (7, 7, 7^\ell)$ for any positive integer ℓ . To see how it works, first consider a complementary array set with $(M, N, L) = (1, 1, 1)$ (a single-point array). Taking the union of seven such array sets as in Remark 4 leads to an array set with $(M, N, L) = (7, 1, 1)$. Then, applying Theorem 3 once leads to an array set with $(M, N, L) = (7, \text{lcm}(7, 1), 7 \times 1) = (7, 7, 7)$. Further applications of Theorem 3 will increase L , but not M, N . The design could also be illustrated by Fig. 15.

3. URA, HURA, AND MURA BASED ON PERIODIC AUTOCORRELATION

In this section, we review related works on URAs, including hexagonal uniformly redundant arrays (HURAs) and modified uniformly redundant arrays (MURAs).

A. URA

We first introduce the concept of periodic autocorrelation and “pseudonoise” that are important to the design of URAs.

Definition 6 Let $C = \{C[i_1, \dots, i_n]\}$ be an **infinite array** on an integer lattice, which satisfies

$$C[i_1, \dots, i_n] = C[I_1, \dots, I_n],$$

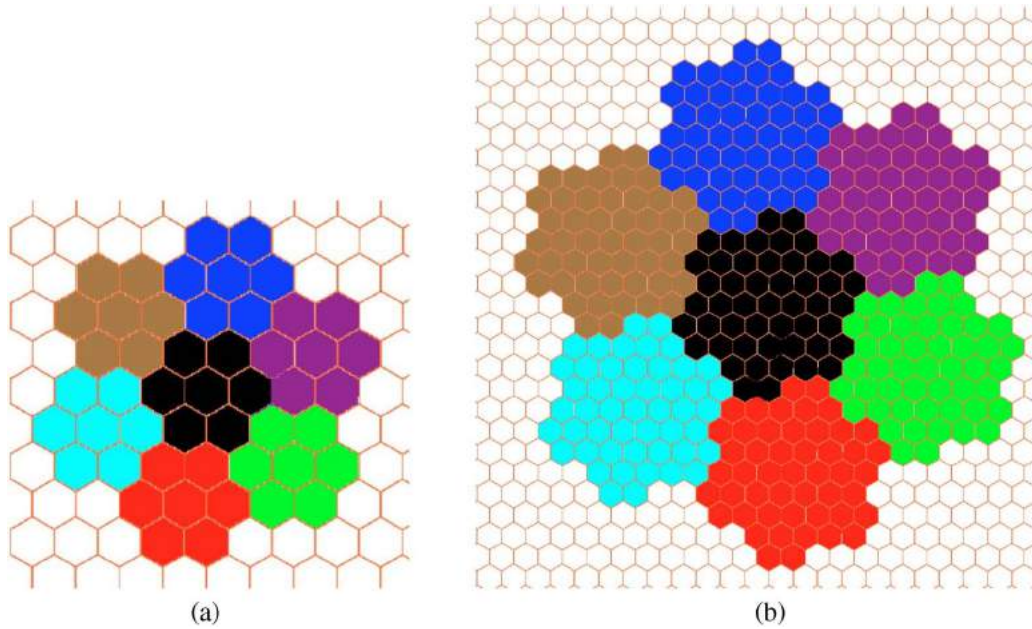


Fig. 15. Complementary array set with parameter $(M, N) = (7, 42, 7^\ell)$ (Design 6), or $(M, N) = (7, 7, 7^\ell)$ (Design 7) for any positive integer ℓ . (a) Illustration of one of the seven arrays of size 7^2 obtained as a result of applying Theorem 3 to a complementary array set of seven arrays of size 7 (indicated by different colors) once. (b) Illustration of one of the seven arrays of size 7^3 obtained as a result of applying Theorem 3 to a complementary array set of seven arrays of size 7^2 (indicated by different colors) once.

for all $i_j \in \mathbb{Z}$ and $i_j \equiv I_j \pmod{L_j}$, $j = 1, 2, \dots, n$, where $L_1, \dots, L_n, I_1, \dots, I_n \in \mathbb{N}$ and $(I_1, \dots, I_n) \in [0, L_1 - 1] \times \dots \times [0, L_n - 1]$. The finite array within $[0, L_1 - 1] \times \dots \times [0, L_n - 1]$, denoted by c , is called the basic array. C is called the periodic extension of s . The **periodic autocorrelation** function of C (or c) is

$$A^C(v_1, \dots, v_n) = \sum_{\substack{i_1 \in [0, L_1 - 1] \\ \dots \\ i_n \in [0, L_n - 1]}} C[i_1, \dots, i_n] \overline{C[i_1 + v_1, \dots, i_n + v_n]}$$

$v_1, \dots, v_n \in \mathbb{Z}$. The periodic cross-correlation between two arrays are similarly defined.

A section of an infinite array C would be a valid URA aperture, if there exists a finite array D such that $C * D^-$ is a periodic extension of the discrete delta function. For a detailed discussion about the benefits and implementations of periodic extension, please refer to [7].

Definition 7 An array of size $L_1 \times \dots \times L_n$ is a **pseudonoise (PN) array** if

- (1) it is $\{\pm 1\}$ -binary;
- (2) all out-of-phase correlations are -1 , i.e., $A^C(v_1, \dots, v_n) = -1$, where $v_1, \dots, v_n \in \mathbb{Z}$ and $v_j \not\equiv 0 \pmod{L_j}$ for at least one $j \in \{1, 2, \dots, n\}$.

In 1967, Calabro and Wolf [12] showed that a class of two-dimensional PN arrays could be synthesized from quadratic residues. The arrays are of size $p_1 \times p_2$, where p_1, p_2 are any prime numbers satisfying $p_2 - p_1 = 2$:

$$D[i_1, i_2] = \begin{cases} -1 & i_2 \equiv 0 \pmod{p_2} \\ 1 & i_1 \equiv 0 \pmod{p_1}, i_2 \not\equiv 0 \pmod{p_2} \\ (i_1/p_1)(i_2/p_2) & \text{otherwise} \end{cases}$$

where (i/p) , $i \in \mathbb{Z}$ is Legendre operator:

$$(i/p) = \begin{cases} 0 & i \equiv 0 \pmod{p} \\ 1 & \exists x \not\equiv 0 \pmod{p}, \text{ s.t. } i \equiv x^2 \pmod{p} \\ -1 & \text{otherwise.} \end{cases}$$

In 1978, following from the above result, Fenimore and Cannon [7] designed C and D such that $C * D^-$ is a periodic extension of the discrete delta function. The design is given below, where (p_1, p_2) is a twin prime pair. The coding array is C :

$$C[i_1, i_2] = \begin{cases} 1 & (i_1/p_1)(i_2/p_2) = 1 \\ 0 & i_2 \equiv 0 \pmod{p_2} \\ 1 & i_1 \equiv 0 \pmod{p_1}, i_2 \not\equiv 0 \pmod{p_2} \\ 0 & \text{otherwise.} \end{cases} \quad (12)$$

The decoding array of C is D^- , where D is

$$D[i_1, i_2] = \begin{cases} 1 & \text{if } C[i_1, i_2] = 1 \\ -1 & \text{if } C[i_1, i_2] = 0. \end{cases}$$

It is shown that

$$C * D^- = \frac{p_1 p_2 - 1}{2} \delta[\mathbf{r}] \quad (\text{within one period}). \quad (13)$$

URAs can also be designed from maximal-length shift-register sequences or m-sequences [39]. The m-sequence is another class of PN sequences, which have lengths $n = 2^k - 1$ with k being any positive integer. They are sometimes referred to as “PN sequences” [40]. In 1976, MacWilliams and Sloane [40] showed how to obtain PN arrays from m-sequences. Let S be an m-sequence of length $n = 2^k - 1$. If $n = n_1 n_2$ such that n_1 and n_2 are relatively prime, a PN array, denoted by H , is designed below:

$$H[i_1, i_2] = S[i], \quad (14)$$

where $i \equiv i_1 \pmod{n_1}$, $0 \leq i_1 < n_1$, and $i \equiv i_2 \pmod{n_2}$, $0 \leq i_2 < n_2$. We note that when $\text{sum}(H) = -1$ [40, Property IP-IV*], we can design a URA with coding array $C = (-H + J)/2$ and decoding array $D = -H^-$ on integer lattices, where J is a unit array, i.e., with all elements equal to one.

B. HURA

In 1985, Finger and Prince [16] designed a class of linear URAs, i.e., sequences C and D such that $C * D$ is a periodic extension of the discrete delta function. The design is based on PN sequences, which in turn come from quadratic residues. Then, by mapping linear sequences onto hexagonal lattice, they proposed the HURAs. In the first step, they constructed the following sequence of length p , where $p \equiv 3 \pmod{4}$ is a prime:

$$D[i] = \begin{cases} 1 & \text{if } i = 0 \\ -(i/p) & \text{otherwise.} \end{cases}$$

Let $C = (D + J)/2$. Then the following identity holds:

$$C * D^- = \frac{p+1}{2} \delta[r] \quad (\text{within one period}). \quad (15)$$

In the second step, they map the sequence D onto a hexagonal lattice:

$$H[i_1 \mathbf{e}_1 + i_2 \mathbf{e}_2] = D[i_1 + \tau i_2], \quad (16)$$

where τ is an integer to be chosen. H is called the Skew-Hadamard URA. It is easy to see that the correlation between H and $(H + J)/2$ is a multiple of the discrete delta function, just like the one-dimensional case.

As to the choice of lattice and τ , it is well stated by [16] that “The freedom available in this procedure rests in the choice of the lattice, the choice of the order p , and the choice of the multiplier τ . The lattice type will determine what symmetries can occur ... The multiplier τ determines the periods of the URA and hence the shape of the basic pattern.” Furthermore, HURAs are those with hexagonal basic patterns, when the lattice is chosen to be hexagonal. The qualified p is either 3 or primes of the form $12k + 1$ [16].

Besides the fact that HURAs are based on hexagonal lattices, they are antisymmetric upon 60 deg rotation. This property provides for effective reduction of background noise [1,2]. Due to similar reasoning, the designs proposed in Section 2 also obtain robustness against background noise.

C. MURA

It has been shown that PN sequences, together with the URAs and HURAs that are based on them, could be made with prime lengths of the form $4k + 3$. Gottesman and Fenimore [17] proposed the MURAs, which further increased the available patterns for CAI. MURAs exist in lengths $p = 4k + 1$, where p is a prime.

The design of MURAs also starts with a sequence D , which is then mapped onto a hexagonal lattice, following the same procedure as HURAs. Recalling URA and HURA designs from Subsections 3.A and 3.B, we design using the following procedure.

Step 1. Let D be a PN sequence (array);

Step 2. Let the coding array C be $(D + J)/2$, and the decoding array be D^- ;

Step 3. (optional) We map sequences onto a two-dimensional lattice [see Eqs. (14) and (16)].

However, the design of MURAs is less straightforward, because D is not a PN sequence and $C \neq (D + J)/2$. One way to design MURA sequences is

$$C[i] = \begin{cases} 0 & i \equiv 0 \pmod{p} \\ 1 & \exists x \not\equiv 0 \pmod{p}, \text{ s.t. } i \equiv x^2 \pmod{p}, \\ 0 & \text{otherwise} \end{cases}$$

$$D[i] = \begin{cases} 1 & i \equiv 0 \pmod{p} \\ 1 & C[i] = 1, i \not\equiv 0 \pmod{p} \\ -1 & \text{otherwise.} \end{cases}$$

It is easy to verify that for any $v \not\equiv 0 \pmod{p}$, we have

$$\sum_{i=0}^{p-1} C(i)D(i+v) = 0. \quad (17)$$

Gottesman and Fenimore [17] also gave a class of MURAs for integer lattices. The coding array is the same as Eq. (12), except for a change of the size: $p_1 = p_2 = p$. The decoding array is D^- , where

$$D[i_1, i_2] = \begin{cases} 1 & i_1 + i_2 \equiv 0 \pmod{p} \\ 1 & C[i_1, i_2] = 1, i_1 + i_2 \equiv 0 \pmod{p} \\ -1 & \text{otherwise.} \end{cases}$$

4. NEW URA CONSTRUCTIONS

A. URA from Periodic Complementary Sequence Set

In this section, we first briefly summarize some similarities and differences between the aperiodic-based and periodic-based designs of CAI, and then propose a new design framework that is based on periodic autocorrelation.

In the aperiodic case, the elements of arrays are assumed to extend only over some finite area and be zero outside that area. This fact provides great convenience for the design of complementary array sets/banks, since several arrays could be easily concatenated while maintaining the unimodular alphabet during the “growth” process. In addition, the concept of “bank” and a growth scheme make the aperiodic-based designs more flexible. For example, we have shown how to make CAI aperture with arbitrary patterns. In the periodic case, the arrays were assumed to be periodic and infinite in extent. The resulting correlations are calculated over a full period. The usual way to design is to first design sequences with good autocorrelation property, e.g., pseudonoise, and then map them onto arrays. As to practical implementations, periodic-based designs often require the physical coding aperture to be periodic extensions of some basic patterns to mimic the periodicity, while aperiodic-based ones do not.

Despite their differences in principles and implementations, the idea of “complementary” can also be associated with periodic correlations, leading to the following concept that is similar to complementary array sets in Section 2.

Definition 8 A set of arrays with the same basic pattern is a periodic complementary array set (PCAS), if the sum of their periodic autocorrelations is a periodic extension of the discrete delta function. A one-dimensional PCAS is also referred to as a periodic complementary sequence set (PCSS). The notation “design parameters” (M, N) or (M, N, L) is similarly defined as in Subsection 2.D.

As discussed before, URAs (including HURAs) require the lengths of sequences to be prime numbers or $2^k - 1$, so the possible sizes of URA arrays are quite limited. However, the above concept produces more admissible lengths, offering more choices in selecting an aperture. For example, we can construct the following URA sequence of length 6.

Example. PCSS with parameter $(M, N, L) = (4, 2, 6)$:

$$\begin{aligned} S_1 &= \{1, -1, -1, -1, -1, -1\}, \\ S_2 &= \{1, 1, 1, 1, -1, -1\}, \\ S_3 &= \{-1, 1, -1, 1, -1, -1\}, \\ S_4 &= \{-1, -1, 1, 1, -1, 1\}. \end{aligned}$$

Then, the sequences are mapped onto a two-dimensional lattice, following procedures similar to Eqs. (14) and (16). Now a natural question that arises is: for a given alphabet, what are the possible lengths for which there exists a PCSS? and how to design them? This will be addressed in the remaining sections.

A natural way to construct a PCSS is to synthesize them from existing designs. Some synthesis methods have been provided for binary PCSS in [41], and they could be easily extended to the nonbinary case. In the following two sections, we propose some different synthesis methods.

At the end of this subsection, there are two remarks worth mentioning. First, the concept of PCSS is not new. It was once referred to as “periodic complementary sequences” or “periodic complementary binary sequences” [41]. To the best of our knowledge, prior works mainly focused on the binary case. One possible reason is its intimate relationship with cyclic difference sets [42]. Second, complementary sequence sets are subclasses of PCSS due to the following fact:

$$A_p^S(v) = A_a^S(v) + A_a^S(v - L) \quad \forall v \in \mathbb{Z}, 0 \leq v < L, \quad (18)$$

where S is a sequence of length L , and $A_p(\cdot)$ and $A_a(\cdot)$ respectively denote periodic and aperiodic autocorrelations.

B. Synthesis Methods from the Chinese Remainder Theorem

1. PCAS Synthesized from PCSS and Perfect Sequence

A sequence is called a “perfect sequence” if its periodic autocorrelation is a periodic extension of the discrete delta function. Consider a PCSS $\{S_m\}_{m=1}^M$ of length s , and a perfect sequence S of length t . We can then construct a PCAS $\{C_m\}_{m=1}^M$ of size $s \times t$ (or similarly $t \times s$):

$$C_m[i, j] = S_m[i]S[j], \quad m = 1, \dots, M, i, j \in \mathbb{Z}. \quad (19)$$

Proof: The periodic autocorrelation of C_m satisfies

$$A^{C_m}(v_1, v_2) = A^{S_m}(v_1)A^S(v_2).$$

Thus, for any $v_1, v_2 \in \mathbb{Z}, (v_1, v_2) \neq (0, 0)$,

$$\sum_{m=1}^M A^{C_m}(v_1, v_2) = \left(\sum_{m=1}^M A^{S_m}(v_1) \right) A^S(v_2) = 0.$$

2. PCSS Synthesized from PCSS and Perfect Sequence

Consider a PCSS $\{S_m\}_{m=1}^M$ of length s , and a perfect sequence S of length t . Also assume that s and t are coprime. We can then construct a PCSS $\{\tilde{S}_m\}_{m=1}^M$ of length st :

$$\tilde{S}_m[i] = C_m[i \bmod s, i \bmod t], \quad i \in \mathbb{Z}, \quad (20)$$

where $\{C_m\}$ is given in Subsection 4.B.1.

Proof: Equation (20) provides a one-to-one mapping between a sequence and an array, guaranteed by the Chinese remainder theorem. The mapping is linear so that the autocorrelation function is preserved, i.e.,

$$A^{\tilde{S}_m}(v) = A^{C_m}(v \bmod s, v \bmod t),$$

and thus the sequence set $\{\tilde{S}_m\}_{m=1}^M$ is complementary.

3. PCSS/PCAS from Two PCSSs with Coprime Lengths

Consider a PCSS $\{S_{m_1}\}_{m_1=1}^{M_1}$ of length s , and another PCSS $\{T_{m_2}\}_{m_2=1}^{M_2}$ of length t . We can then construct a PCAS $\{C_{(m_1, m_2)}\}$ of size $s \times t$:

$$C_{(m_1, m_2)}[i, j] = S_{m_1}[i]T_{m_2}[j] \quad (21)$$

where $m_1 = 1, \dots, M_1, m_2 = 1, \dots, M_2$, and $i, j \in \mathbb{Z}$. Further, if s and t are coprime, we can construct a PCSS of length st .

Proof: For a given $1 \leq m_2 \leq M_2$,

$$\sum_{m_1=1}^{M_1} A^{C_{(m_1, m_2)}}(v_1, v_2) = \begin{cases} s \cdot A^{T_{m_2}}(v_2) & v_1 = 0 \\ 0 & \text{otherwise.} \end{cases}$$

Thus, for $v_1, v_2 \in \mathbb{Z}, (v_1, v_2) \neq (0, 0)$,

$$\sum_{m_2=1}^{M_2} \sum_{m_1=1}^{M_1} A^{C_{(m_1, m_2)}}(v_1, v_2) = \sum_{m_2=1}^{M_2} \left(\sum_{m_1=1}^{M_1} A^{C_{(m_1, m_2)}}(v_1, v_2) \right) = 0.$$

If s and t are coprime, a PCSS could be designed using the mapping given in Eq. (20).

Remark 8 This result is stronger than that given in [41, Theorem 6], since it does not require the number of sequences to be relatively prime.

4. PCAS Constructed from Another PCAS of a Different Size

Assume that we have a PCAS of size $s \times t$ synthesized from PCSS $\{S_{m_1}\}_{m_1=1}^{M_1}$ and $\{T_{m_2}\}_{m_2=1}^{M_2}$ using the method in Subsection 4.B.3. Suppose that $\gcd(s, t) \neq 1$, but $s = s_1 s_2$ for some $s_1 \neq 1$ and $s_2 \neq 1$, where $\gcd(s_1, s_2) = \gcd(s_2, t) = 1$. A PCAS of size $s_1 \times s_2 t$ could be designed by first mapping the PCSS $\{S_{m_1}\}_{m_1=1}^{M_1}$ to a PCAS of size $s_1 \times s_2$ in a way similar to Eq. (19), then constructing a three-dimensional PCAS of size $s_1 \times s_2 \times t$ in a way similar to Eq. (19), and finally mapping the latter two dimensions to a single dimension in a way similar to Eq. (20), resulting in a PCAS of size $s_1 \times s_2 t$.

C. Synthesis via Unitary Matrices

Theorem 5 For any positive integer s , there exists at least one PCSS with design parameters $(M, N, L) = (p_n, p_1 \cdots p_n, s)$, where $p_1 < \cdots < p_n$ are all the distinct prime divisors of s .

For any positive integers s_1, \dots, s_k , there exists at least one PCAS of size $s_1 \times \cdots \times s_k$ with design parameters $(M, N, L) = (p_n, p_1 \cdots p_n, st)$, where $p_1 < \cdots < p_n$ are all the distinct prime divisors of $s_1 \cdots s_k$.

The proof is included in Appendix C.

Remark 9 Theorem 5 gives the construction for PCAS of an arbitrary size, where the alphabet is determined by the product of the distinct prime divisors of the size, and the order is the largest prime divisor. From the proof of Theorem 5, the result also holds for aperiodic autocorrelations.

A natural question that arises is how tight the result in Theorem 5 is. Specifically, is there any solution whose order N is less than p_n ? This is clearly not the case for Golay complementary sequence pair, where the size s is a power of 2. Although we were not able to answer this question in general, we were able to prove the following results.

Theorem 6 For any prime number p , a p -regular set, denoted by $RC^{(p)}$, is defined to be a set of p distinct unimodular complex numbers that form the vertices of a uniform polygon in the complex plane. Let $N = p_1^{r_1} \cdots p_n^{r_n}$, $r_j \geq 1$ be a positive integer with distinct prime divisors $p_j, j = 1, \dots, n$. Consider M variables x_1, \dots, x_M that take values in the set of N th root of unity. Suppose that $\sum_{m=1}^M x_m = 0$.

1. If $n \leq 2$, the set $\{x_m\}_{m=1}^M$ can be written as the unions of p_k -regular configurations, i.e.,

$$\{x_1, \dots, x_M\} = \bigcup_{\{(k,j)|c_k>0, k=1, \dots, n, j=1, \dots, c_k\}} RC_j^{(p_k)}. \quad (22)$$

2. If $n \leq 2$, M can be written as

$$M = c_1 p_1 + \cdots + c_n p_n, \quad (23)$$

where c_1, \dots, c_n are nonnegative integers.

The proof is given in Appendix D.

Remark 10 Consider an aperiodic complementary array set $\{S_m\}_{m=1}^M$ with design parameters (M, N, L) . Then we have $\sum_{m=1}^M S_m[0]S_m[L-1] = 0$. Assume that the alphabet is N -phase, where $N = p_1^{r_1}$ ($n = 1$) or $N = p_1^{r_1} p_2^{r_2}$ with p_1 and p_2 distinct primes ($n = 2$). Applying Theorem 6, Eq. (23) implies that (1) $M \geq p_1$ if $n = 1$; (2) $M \geq \min\{p_1, p_2\}$ if $n = 2$. Due to similar reasons, $M = 7$ in Design 7 is tight whenever N is a power of 7.

5. SIMULATION RESULTS

We have performed computer simulations to demonstrate a multichannel CAI system and a classical URA-based one.

The multichannel CAI system that we select comes from Design 2. Admittedly, in practice we only need four pairs of aperture arrays with $\{-1, 1\}$ -alphabet. But the coded images contain negative entries, which are not straightforward to illustrate by simulation (we used MATLAB software). We thus provide an alternative approach, which relies on the following lemma.

Lemma 2 Suppose that $\{(C_m, D_m)\}_{m=1}^M$ is a complementary bank with alphabet $\mathfrak{A} = \{-1, 1\}$ and it satisfies $\sum_{m=1}^M D_m = 0$. Then $\{(\tilde{C}_m, D_m)\}_{m=1}^M$ is a complementary bank, where $\tilde{C}_m = (C_m + J)/2$, $m = 1, \dots, M$. Here, 0 and J respectively denote the array of zeros and the array of ones, whose supports are the same as D_m .

Proof 2 The proof follows immediately from

$$\begin{aligned} \sum_{m=1}^M \tilde{C}_m * D_m^- &= \sum_{m=1}^M \frac{1}{2} (C_m + J) * D_m^- \\ &= \frac{1}{2} \sum_{m=1}^M C_m * D_m^- + \frac{1}{2} J * \left(\sum_{m=1}^M D_m \right)^- \\ &= \frac{1}{2} \sum_{m=1}^M C_m * D_m^-. \end{aligned} \quad (24)$$

The above result gives a general method to design a mask with simple closing/opening pinholes (the elements of C are either 0 or 1). In practice, the method is of interest on its own right, but we do not elaborate here. As a corollary of Lemma 2, it is easy to see that if $\{C_m\}_{m=1}^M$ is a complementary array set with alphabet $\mathfrak{A} = \{-1, 1\}$, then

$$\left\{ \left(\frac{1}{2} (C_m + J), C_m \right) \right\}_{m=1}^M \cup \left\{ \left(\frac{1}{2} (-C_m + J), -C_m \right) \right\}_{m=1}^M$$

is a complementary bank.

Following Design 2 and the above result, we obtain the following eight-channel CAI $\{(C_m, D_m)\}_{m=1}^8$, each with a mask as shown in Fig. 5. The coding arrays are

$$\begin{aligned} \{C_1[k]\}_{k=0}^6 &= \{1, 1, 0, 1, 1, 0, 1\}, \\ \{C_2[k]\}_{k=0}^6 &= \{0, 1, 1, 0, 0, 1, 1\}, \\ \{C_3[k]\}_{k=0}^6 &= \{1, 1, 0, 1, 0, 1, 1\}, \\ \{C_4[k]\}_{k=0}^6 &= \{1, 1, 1, 0, 1, 0, 1\}, \\ \{C_5[k]\}_{k=0}^6 &= \{0, 0, 1, 0, 0, 1, 0\}, \\ \{C_6[k]\}_{k=0}^6 &= \{1, 0, 0, 1, 1, 0, 0\}, \\ \{C_7[k]\}_{k=0}^6 &= \{0, 0, 1, 0, 1, 0, 0\}, \\ \{C_8[k]\}_{k=0}^6 &= \{0, 0, 0, 1, 0, 1, 0\}. \end{aligned}$$

If we choose the element labeled 0 to be the origin, the decoding arrays are

$$\begin{aligned} \{D_1[k]\}_{k=0}^6 &= \{1, 1, -1, 1, 1, -1, 1\}, \\ \{D_2[k]\}_{k=0}^6 &= \{-1, -1, 1, 1, 1, 1, -1\}, \\ \{D_3[k]\}_{k=0}^6 &= \{1, -1, 1, 1, 1, -1, 1\}, \\ \{D_4[k]\}_{k=0}^6 &= \{1, 1, -1, 1, 1, 1, -1\}, \\ \{D_5[k]\}_{k=0}^6 &= \{-1, -1, 1, -1, -1, 1, -1\}, \\ \{D_6[k]\}_{k=0}^6 &= \{1, 1, -1, -1, -1, -1, 1\}, \\ \{D_7[k]\}_{k=0}^6 &= \{-1, 1, -1, -1, -1, 1, -1\}, \\ \{D_8[k]\}_{k=0}^6 &= \{-1, -1, 1, -1, -1, -1, 1\}. \end{aligned}$$

Figure 17 illustrates how a source object is coded and decoded in a multichannel system. The source object is a 130×130

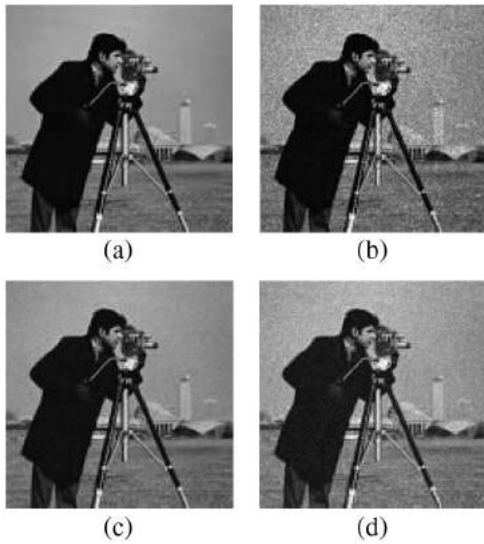


Fig. 16. Comparison of (a) the source image, (b) the image from a single pinhole, (c) the image from the multichannel CAI system, and (d) the image from the URA-based CAI system, under Poisson noises.

pixels “camera man” image and the distance between two pinholes is 60 pixels. The gray level is normalized to be in the range of [0, 255]. It is worth mentioning that the bright (white) part of the images produced by MATLAB (as shown in Figs. 16–18) corresponds to low light intensity in the real world.

The second simulation is for URAs (shown in Fig. 18). It uses the same source object and following aperture:

$$\begin{bmatrix} 0 & 1 & 1 & 1 & 1 \\ 0 & 0 & 1 & 1 & 0 \\ 0 & 1 & 0 & 0 & 1 \end{bmatrix}, \quad (25)$$

which is a 3×5 array that comes from the m-sequence of length 15 (see Subsection 3.A for details). In the implementation, we use the arrangement suggested by [7], i.e., a 6×10 aperture composed of a periodic extension of the basic 3×5 patterns (with 32 open pinholes), and a 3×5 decoding array.

Next, we repeat the experiment by taking noises into account. We first assume additive noises that follow independent Poisson distributions. In other words, the recorded image at the k th pinhole of the coding aperture is $O + n_k$, where O and n_k respectively denote the array of source image and noises, and each pixel $n_k[i, j]$ is an independent Poisson random variable with rate (expectation) λ . For each λ , we obtain the reconstructed 130×130 images from the multichannel CAI system [the bottom-right of Fig. 17(b)] and from the URA-based CAI system [the center of Fig. 18(b)], denoted respectively by \hat{O}_m, \hat{O}_u . Then we compute the log of SNR ratio $s_m = \log(\|O\|_F^2 / \|\hat{O}_m - O\|_F^2)$, $s_u = \log(\|O\|_F^2 / \|\hat{O}_u - O\|_F^2)$ (where $\|\cdot\|_F$ denotes the Frobenius norm) based on the average of 20 independent repetitions. (In the computation, we have normalized the pixel values to the range [0, 1], with 0 and 1 respectively denoting the lowest intensity and the highest intensity.) We repeat the experiment for $\lambda = 10, 20, 30, 40, 50$, and obtain $s_m/s_u = 6.1/6, 5/4.8, 4.3/4.2, 3.8/3.7, 3.5/3.3$, respectively. This result shows that the eight-channel CAI with

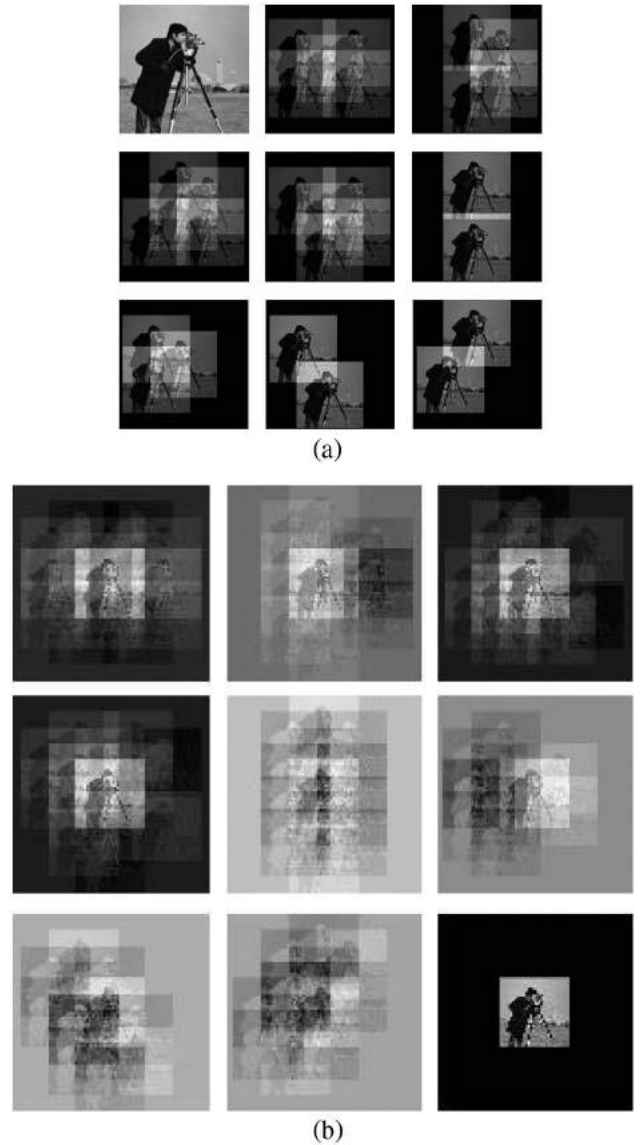


Fig. 17. Demonstration of the encoding and decoding process of a multichannel CAI system. (a) The upper-left image, “cameraman,” is the source image. From the upper-middle to the bottom-right, the images are the coded images from apertures C1, ..., C8 in each channel. (b) From the upper-left to the bottom-middle, the images are the decoded results from D1, ..., D8 in each channel. The bottom-right image is the reconstructed image, coming from the addition of the eight decoded results.

28 open pinholes achieves better SNR gain compared to the URA with 32 open pinholes.

It is usually more reasonable to assume that the noise is signal dependent, especially in our “cameraman” example where there is a significant part of low-intensity background. We thus repeat the experiment by assuming photon noise, also known as Poisson noise. In other words, the recorded image at the k th pinhole of the coding aperture is $O + n_k$, whose $[i, j]$ th pixel is an independent Poisson random variable with rate $O[i, j]$. We repeat the experiment 20 times and obtain the average log SNR $s_m = 6.2920$, $s_u = 5.2781$. The result shows that the eight-channel CAI achieves much better SNR even though

it uses only 28 open pinholes, compared with the URA-based design. For illustration purpose, Fig. 16 plots the source image, the recorded image from a single pinhole, the reconstructed image from the eight-channel CAI system, and the image from the URA-based one, under signal-dependent Poisson noises in one experiment.

6. CONCLUSION

In this work, two classes of coded aperture imaging systems are studied that are constructed based on aperiodic or periodic correlations. For the first case, we extended the concept of Golay complementary array pairs to complementary array sets and complementary array banks on lattices. Under the general framework, we provided methods and examples for the design of the complementary arrays. The findings not only lead to more flexible and robust designs of the coded aperture imaging systems, but also bring new theoretical insights. For the second case, we reviewed the state-of-the-art URA designs and further proposed some new classes of the URA designs. Simulation results are provided to demonstrate our proposed scheme.

APPENDIX A: PROOF OF THEOREM 1

The following lemmas are helpful to the proof of Theorem 1.

Lemma 3 *If complex numbers $\alpha_1, \dots, \alpha_4$ are unimodular and satisfy $\sum_{k=1}^4 \alpha_k = 0$, then they contain two opposite pairs.*

Proof of Lemma 3:

Let $y = \alpha_1 + \alpha_2$, $z = (-\alpha_3) + (-\alpha_4)$, then $y = z$. Because $|\alpha_1| = |\alpha_2| = 1$, y is on the bisector of α_1 and α_2 . Similarly, z is on the bisector of $-\alpha_3$ and $-\alpha_4$. Since $y = z$, we have $\alpha_1 = -\alpha_3$ or $\alpha_1 = -\alpha_4$.

Lemma 4 *If roots of unity α_1, α_2 satisfy $|\alpha_1 - 2\alpha_2| = 1$, then $\alpha_1 = \alpha_2$.*

Proof of Lemma 4:

The identity $1 = (\alpha_1 - 2\alpha_2)(\bar{\alpha}_1 - 2\bar{\alpha}_2) = 1 - 2(\alpha_1\bar{\alpha}_2 + \bar{\alpha}_1\alpha_2) + 4$ implies $\alpha_1\bar{\alpha}_2 = 1$, i.e., $\alpha_1 = \alpha_2$.

Proof of Theorem 1:

Assume that there exists a complementary array pair. Writing down (2) explicitly we obtain the following system of equations consisting of nine equations and 14 variables $\{x_k\}_{k=0}^6 \cup \{y_k\}_{k=0}^6$:

$$x_1\bar{x}_3 + x_6\bar{x}_4 + y_1\bar{y}_3 + y_6\bar{y}_4 = 0, \quad (\text{A1})$$

$$x_0\bar{x}_1 + x_3\bar{x}_2 + x_5\bar{x}_6 + x_4\bar{x}_0 + y_0\bar{y}_1 + y_3\bar{y}_2 + y_5\bar{y}_6 + y_4\bar{y}_0 = 0, \quad (\text{A2})$$

$$x_1\bar{x}_4 + y_1\bar{y}_4 = 0, \quad (\text{A3})$$

$$x_2\bar{x}_4 + x_1\bar{x}_5 + y_2\bar{y}_4 + y_1\bar{y}_5 = 0, \quad (\text{A4})$$

$$x_0\bar{x}_2 + x_6\bar{x}_1 + x_4\bar{x}_3 + x_5\bar{x}_0 + y_0\bar{y}_2 + y_6\bar{y}_1 + y_4\bar{y}_3 + y_5\bar{y}_0 = 0, \quad (\text{A5})$$

$$x_2\bar{x}_5 + y_2\bar{y}_5 = 0, \quad (\text{A6})$$

$$x_3\bar{x}_5 + x_2\bar{x}_6 + y_3\bar{y}_5 + y_2\bar{y}_6 = 0, \quad (\text{A7})$$

$$x_0\bar{x}_3 + x_1\bar{x}_2 + x_5\bar{x}_4 + x_6\bar{x}_0 + y_0\bar{y}_3 + y_1\bar{y}_2 + y_5\bar{y}_4 + y_6\bar{y}_0 = 0, \quad (\text{A8})$$

$$x_3\bar{x}_6 + y_3\bar{y}_6 = 0. \quad (\text{A9})$$

We only need to prove that the above system of equations have no solution on the unit circle. Assume without loss of generality that $x_1 = y_1 = 1$. After simplifying Eqs. (A3), (A1), (A6), and (A9) we have

$$y_4 = -x_4, \quad (\text{A10})$$

$$y_3 = -(x_3 + (\bar{x}_6 - \bar{x}_4)x_4) = -x_3 - \bar{x}_6x_4 + 1, \quad (\text{A11})$$

$$y_5 = -\bar{x}_2x_5y_2, \quad (\text{A12})$$

$$y_6 = -\bar{x}_3x_6y_3. \quad (\text{A13})$$

From Eq. (A11), we obtain $y_3 + x_3 + \bar{x}_6x_4 - 1 = 0$. Due to Lemma 3, we have three cases to consider:

Case A: $y_3 = 1$, $x_4 = -x_3x_6$; Case B: $x_3 = 1$, $y_3 = -x_4\bar{x}_6$; Case C: $x_6 = x_4$, $y_3 = -x_3$.

Case A: $y_3 = 1$, $x_4 = -x_3x_6$

From Eqs. (A10), (A12), and (A13), we eliminate variables x_4, y_3, y_4, y_5, y_6 in Eqs. (A4) and (A7) and obtain

$$-x_2\bar{x}_3\bar{x}_6 + \bar{x}_5 + \bar{x}_3\bar{x}_6y_2 - x_2\bar{x}_5\bar{y}_2 = 0, \quad (\text{A14})$$

$$x_3\bar{x}_5 + x_2\bar{x}_6 - x_2\bar{x}_5\bar{y}_2 - x_3\bar{x}_6y_2 = 0. \quad (\text{A15})$$

We write Eqs. (A14) and (A15) as

$$x_5\bar{x}_3(x_2 - y_2) = x_6(1 - x_2\bar{y}_2), \quad (\text{A16})$$

$$x_5(\bar{x}_3 - \bar{x}_2y_2) = x_6(\bar{x}_3\bar{y}_2 - \bar{x}_2). \quad (\text{A17})$$

If $x_2 \neq y_2$, Eq. (A16) gives

$$x_5 = x_3 \frac{1 - x_2\bar{y}_2}{x_2 - y_2} x_6 = -x_3\bar{y}_2x_6.$$

If $x_2 \neq x_3y_2$, Eq. (A17) gives

$$x_5 = \frac{\bar{x}_3\bar{y}_2 - \bar{x}_2}{\bar{x}_3 - \bar{x}_2y_2} x_6 = \bar{y}_2x_6.$$

So there are four cases to consider that further eliminate the variables.

Case A1: $x_5 = -x_3\bar{y}_2x_6$, $x_5 = \bar{y}_2x_6$

Clearly, $x_3 = -1$. Eliminating variables in Eqs. (A2) and (A8) we obtain

$$(x_0 - \bar{x}_2 - \bar{x}_2 - x_6\bar{y}_0) + (\bar{y}_2 + x_6\bar{x}_0 + y_0 + \bar{y}_2) = 0,$$

$$-(x_0 - \bar{x}_2 - \bar{x}_2 - x_6\bar{y}_0) + (\bar{y}_2 + x_6\bar{x}_0 + y_0 + \bar{y}_2) = 0,$$

which is equivalent to

$$x_0 - \bar{x}_2 - \bar{x}_2 - x_6\bar{y}_0 = 0, \quad (\text{A18})$$

$$\bar{y}_2 + x_6\bar{x}_0 + y_0 + \bar{y}_2 = 0. \quad (\text{A19})$$

We further obtain

$$y_0 = x_6(\bar{x}_0 - 2x_2), \quad (\text{A20})$$

$$y_2 = \bar{x}_6(\bar{x}_2 - x_0). \quad (\text{A21})$$

Equation (A20) gives $|\bar{x}_0 - 2x_2| = 1$, which further implies that $\bar{x}_0 = x_2$. This is a contradiction to Eq. (A21).

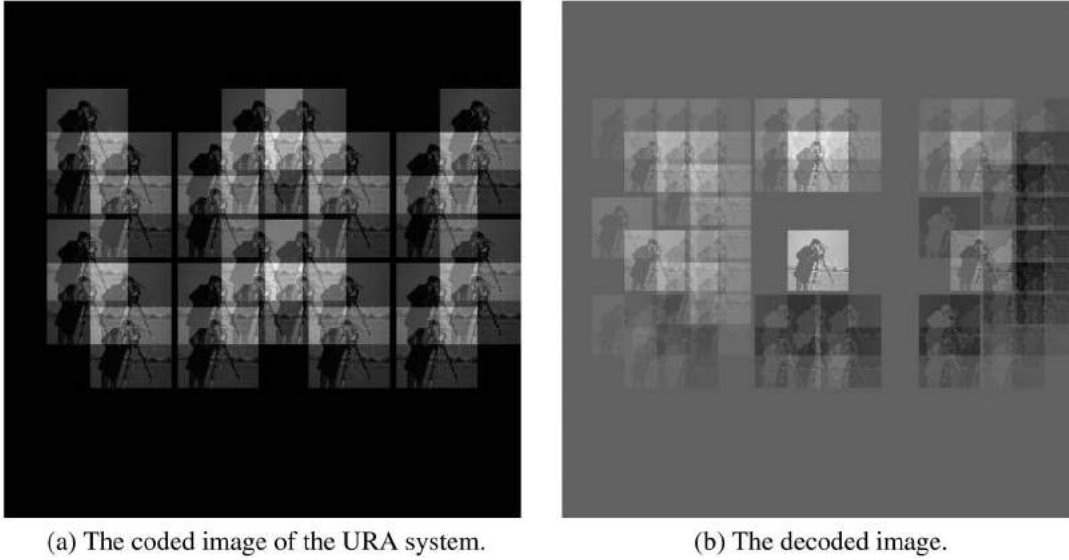


Fig. 18. Demonstration of the encoding and decoding process of a URA-based CAI system: the coded aperture produces a cyclic version of the basic aperture pattern in (a), from which the source image is reconstructed in the center area in (b).

Case A2: $x_2 = y_2, x_5 = \bar{y}_2 x_6$

We only need to check the validity of Eqs. (A2), (A5), and (A8). We write them in terms of five variables x_0, x_2, x_3, x_6, y_0 :

$$x_0 + x_3 \bar{x}_2 + \bar{x}_2 - x_3 x_6 \bar{x}_0 + y_0 + \bar{x}_2 + \bar{x}_2 x_3 + x_3 x_6 \bar{y}_0 = 0, \quad (\text{A22})$$

$$\begin{aligned} x_0 \bar{x}_2 + \bar{x}_2 x_6 \bar{x}_0 + y_0 \bar{x}_2 - \bar{x}_3 x_6 + x_3 x_6 - \bar{x}_2 x_6 \bar{y}_0 &= 0, \\ x_0 + x_3 \bar{x}_2 - \bar{x}_2 + x_3 x_6 \bar{x}_0 + y_0 x_3 + \bar{x}_2 x_3 - \bar{x}_2 - x_6 \bar{y}_0 &= 0. \end{aligned} \quad (\text{A23})$$

In fact, a contradiction can be obtained from Eqs. (A22) and (A23). Taking the sum and difference of the two equations, we obtain

$$(x_3 + 1)y_0 + (x_3 - 1)x_6 \bar{y}_0 = -4\bar{x}_2 x_3 - 2x_0, \quad (\text{A24})$$

$$(x_3 + 1)x_6 \bar{y}_0 - (x_3 - 1)y_0 = -4\bar{x}_2 + 2x_3 x_6 \bar{x}_0. \quad (\text{A25})$$

If we have a valid solution $(x_2, x_3, x_0, y_0, x_6)$, it is easy to see that $(\xi^{-1}x_2, x_3, \xi x_0, \xi y_0, \xi^2 x_6)$ is also a valid solution for any unimodular complex number ξ . Therefore, we only need to consider the case $x_6 = 1$. Replacing $x_6 = 1$ into Eq. (A25), multiplying the equation with $-\bar{x}_3$, and then taking the conjugate, we obtain

$$-(x_3 + 1)y_0 - (x_3 - 1)\bar{y}_0 = 4x_2 x_3 - 2x_0. \quad (\text{A26})$$

Adding Eqs. (A24) and (A26) gives

$$x_0 = (x_2 - \bar{x}_2)x_3. \quad (\text{A27})$$

From the identity $1 = |x_0| = |x_2 - \bar{x}_2||x_3| = |x_2 - \bar{x}_2|$, x_2 is in the form of

$$\frac{\sqrt{3}}{2}\delta_1 + \frac{i}{2}\delta_2, \quad \delta_1, \delta_2 \in \{1, -1\}. \quad (\text{A28})$$

Combining Eqs. (A28) and (A27) gives $x_0 = i\delta_2 x_3$. Furthermore, Eq. (A24) is simplified to be

$$(x_3 + 1)y_0 + (x_3 - 1)\bar{y}_0 = -2\sqrt{3}\delta_1 x_3. \quad (\text{A29})$$

Equation (A29) implies that

$$\begin{aligned} 2\sqrt{3} &= |(x_3 + 1)y_0 + (x_3 - 1)\bar{y}_0| \leq |x_3 + 1| + |x_3 - 1| \\ &\leq 2\sqrt{2}, \end{aligned}$$

which is a contradiction.

Case A3: $x_5 = -x_3 \bar{y}_2 x_6, x_2 = x_3 y_2$

First, we rewrite Eqs. (A2) and (A8) in terms of x_0, x_3, x_6, y_0, y_2 :

$$x_0 + 2\bar{y}_2 - 2x_3 \bar{y}_2 - x_3 x_6 \bar{x}_0 + y_0 + x_3 x_6 \bar{y}_0 = 0, \quad (\text{A30})$$

$$x_0 \bar{x}_3 + 2\bar{x}_3 \bar{y}_2 + 2\bar{y}_2 + x_6 \bar{x}_0 + y_0 - \bar{x}_3 x_6 \bar{y}_0 = 0. \quad (\text{A31})$$

If we have a valid solution $(y_2, x_3, x_0, y_0, x_6)$, it is easy to see that $(\xi^{-1}y_2, x_3, \xi x_0, \xi y_0, \xi^2 x_6)$ is also a valid solution for any unimodular complex number ξ . Therefore, we only need to consider the case $x_6 = 1$. By computing Eq. (A30) $+x_3$, Eq. (A31) and (A30) $-x_3$, Eq. (A31) we obtain

$$(x_3 + 1)y_0 + (x_3 - 1)\bar{y}_0 = -4\bar{y}_2 - 2x_0, \quad (\text{A32})$$

$$-(x_3 + 1)\bar{y}_0 + (x_3 - 1)y_0 = -4x_3 \bar{y}_2 - 2x_3 \bar{x}_0. \quad (\text{A33})$$

Multiplying Eq. (A33) by \bar{x}_3 , and then taking the conjugate, we obtain

$$-(x_3 + 1)y_0 - (x_3 - 1)\bar{y}_0 = -4y_2 - 2x_0. \quad (\text{A34})$$

Adding Eqs. (A32) and (A34) we obtain

$$x_0 = -(y_2 + \bar{y}_2).$$

Thus, y_2 is in the form of

$$y_2 = \frac{1}{2}\delta_1 + \frac{\sqrt{3}i}{2}\delta_2, \quad \delta_1, \delta_2 \in \{1, -1\}.$$

Furthermore,

$$x_0 = -\delta_1,$$

$$(x_3 + 1)y_0 + (x_3 - 1)\bar{y}_0 = -2\sqrt{3}\delta_2,$$

which implies that $2\sqrt{3} \leq 2\sqrt{2}$.

Case A4: $x_2 = y_2$, $x_2 = x_3 y_2$

Similar to Case A1, Eqs. (A2) and (A8) imply

$$-(2\bar{x}_2 + x_0) = y_0, \quad (\text{A35})$$

$$x_5 \bar{x}_6 - x_6 (\bar{x}_0 + x_2) = 0. \quad (\text{A36})$$

Equation (A35) implies that $\bar{x}_2 = -x_0$, which is a contradiction to Eq. (A36).

Case B: $x_3 = 1$, $y_3 = -x_4 \bar{x}_6$

From Eqs. (A4) and (A7), we obtain

$$(\bar{x}_5 - y_2 \bar{x}_4)(1 - x_2 \bar{y}_2) = 0, \quad (\text{A37})$$

$$(x_2 \bar{x}_6 + y_2 \bar{x}_4)(1 + x_4 \bar{x}_5 \bar{y}_2) = 0. \quad (\text{A38})$$

If $y_2 \neq x_4 \bar{x}_5$, Eq. (A37) gives $x_2 = y_2$. If $x_2 \neq -x_6 \bar{x}_4 y_2$, Eq. (A38) gives $x_5 = -x_4 \bar{y}_2$. We therefore have the following four cases to discuss.

Case B1: $y_2 = x_4 \bar{x}_5$, $x_2 = -x_6 \bar{x}_4 y_2 = -x_6 \bar{x}_5$

First, we rewrite Eqs. (A5) and (A8) in terms of x_0 , x_4 , x_5 , x_6 , y_0 :

$$2x_6 - x_0 x_5 \bar{x}_6 + 2x_4 + \bar{x}_4 x_5 y_0 + x_4 x_5 \bar{x}_6 \bar{y}_0 + \bar{x}_0 x_5 = 0, \quad (\text{A39})$$

$$2\bar{x}_4 x_5 + x_0 - 2x_5 \bar{x}_6 - \bar{x}_4 x_6 y_0 + x_4 \bar{y}_0 + \bar{x}_0 x_6 = 0. \quad (\text{A40})$$

If we have a valid solution $(x_0, y_0, x_4, x_6, x_5)$, it is easy to see that $(\xi x_0, \xi y_0, \xi^2 x_4, \xi^2 x_6, \xi^3 x_5)$ is also a valid solution for any unimodular complex number ξ . Therefore, we only need to consider the case $x_6 = 1$. Taking $x_6 = 1$ into Eqs. (A39) and (A40), multiplying Eq. (A40) by $-\bar{x}_5$, and taking its conjugate, we obtain

$$2 - x_0 x_5 + 2x_4 + \bar{x}_4 x_5 y_0 + x_4 x_5 \bar{y}_0 + \bar{x}_0 x_5 = 0, \quad (\text{A41})$$

$$2 - x_0 x_5 - 2x_4 - \bar{x}_4 x_5 y_0 + x_4 x_5 \bar{y}_0 - \bar{x}_0 x_5 = 0. \quad (\text{A42})$$

Adding Eqs. (A41) and (A42) gives

$$4 = 2x_0 x_5 - 2x_4 x_5 \bar{y}_0. \quad (\text{A43})$$

Because $|2x_0 x_5| = |2x_4 x_5 \bar{y}_0| = 2$, the only possibility is

$$x_0 x_5 = 1, x_4 x_5 \bar{y}_0 = -1. \quad (\text{A44})$$

Taking Eqs. (A44) into (A41) we obtain $2x_4 = 0$, which is a contradiction.

Case B2: $x_2 = y_2$, $x_2 = -x_6 \bar{x}_4 y_2$

Clearly, $x_6 = -x_4$. Because $y_3 = -x_4 \bar{x}_6 = 1$, this case is covered by Case A.

Case B3: $y_2 = x_4 \bar{x}_5$, $x_5 = -x_4 \bar{y}_2$

Clearly, $y_2 = -x_4 \bar{x}_5$. Because $y_2 = x_4 \bar{x}_5 = -y_2$, this case is not possible.

Case B4: $x_2 = y_2$, $x_5 = -x_4 \bar{y}_2 = -x_4 \bar{x}_2$

First, we rewrite Eqs. (A2) and (A5) in terms of x_0 , x_2 , x_4 , x_6 , y_0 :

$$2\bar{x}_2 - 2\bar{x}_2 x_4 \bar{x}_6 + x_0 + y_0 + x_4 \bar{x}_0 - x_4 \bar{y}_0 = 0, \quad (\text{A45})$$

$$2x_4 + 2x_6 + x_0 \bar{x}_2 + \bar{x}_2 y_0 - \bar{x}_2 x_4 \bar{x}_0 + \bar{x}_2 x_4 \bar{y}_0 = 0. \quad (\text{A46})$$

If we have a valid solution $(x_2, x_0, y_0, x_4, x_6)$, it is easy to see that $(\xi^{-1} x_2, \xi x_0, \xi y_0, \xi^2 x_4, \xi^2 x_6)$ is also a valid solution for any unimodular complex number ξ . Therefore, we only need to consider the case $x_4 = 1$. Taking the conjugate of Eq. (A45), multiplying Eq. (A46) by \bar{x}_2 , and letting $x_4 = 1$, we have

$$2x_2 - 2x_2 x_6 + \bar{x}_0 + \bar{y}_0 + x_0 - y_0 = 0, \quad (\text{A47})$$

$$2x_2 + 2x_2 x_6 + x_0 + y_0 - \bar{x}_0 + \bar{y}_0 = 0. \quad (\text{A48})$$

Adding Eqs. (A47) and (A48), we obtain

$$4x_2 + 2x_0 + 2\bar{y}_0 = 0. \quad (\text{A49})$$

Because $|4x_2| = 4$, $|2x_0| = |2\bar{y}_0| = 2$, the only possibility is

$$x_0 = -x_2, \quad \bar{y}_0 = -x_2. \quad (\text{A50})$$

Applying Eqs. (A47)–(A50) gives $2x_2 x_6 = 0$, which is a contradiction.

Case C: $x_6 = x_4$, $y_3 = -x_3$

From Eqs. (A4) and (A7), we obtain

$$(\bar{x}_5 - \bar{x}_4 y_2)(1 - x_2 \bar{y}_2) = 0, \quad (\text{A51})$$

$$(\bar{x}_5 x_3 + \bar{x}_4 y_2)(x_2 + y_2) = 0. \quad (\text{A52})$$

If $y_2 \neq x_2$, Eq. (A51) gives $y_2 = x_4 \bar{x}_5$. If $y_2 \neq -x_2$, Eq. (A52) gives $y_2 = -x_3 x_4 \bar{x}_5$. So there are four cases to consider.

Case C1: $y_2 = x_2$, $y_2 = -x_3 x_4 \bar{x}_5$

First, we rewrite Eqs. (A5) and (A8) in terms of x_0 , x_2 , x_3 , x_4 , y_0 :

$$2x_4 + 2\bar{x}_3 x_4 + \bar{x}_2 x_0 + \bar{x}_2 y_0 - \bar{x}_2 x_3 x_4 \bar{x}_0 + \bar{x}_2 x_3 x_4 \bar{y}_0 = 0, \quad (\text{A53})$$

$$2\bar{x}_2 - 2\bar{x}_2 x_3 + \bar{x}_c x_0 - \bar{x}_3 y_0 + x_4 \bar{x}_0 + x_4 \bar{y}_0 = 0. \quad (\text{A54})$$

If we have a valid solution $(x_2, x_3, x_0, y_0, x_4)$, it is easy to see that $(\xi^{-1} x_2, x_3, \xi x_0, \xi y_0, \xi^2 x_4)$ is also a valid solution for any unimodular complex number ξ . Therefore, we only need to consider the case $x_4 = 1$. Taking the conjugate of Eq. (A54), multiplying it by \bar{x}_2 , and letting $x_4 = 1$, Eqs. (A53) and (A54) give

$$2 + 2\bar{x}_3 + \bar{x}_2 x_0 + \bar{x}_2 y_0 - \bar{x}_2 x_3 \bar{x}_0 + \bar{x}_2 x_3 \bar{y}_0 = 0, \quad (\text{A55})$$

$$2 - 2\bar{x}_3 + \bar{x}_2 x_0 + \bar{x}_2 y_0 + \bar{x}_2 x_3 \bar{x}_0 - \bar{x}_2 x_3 \bar{y}_0 = 0. \quad (\text{A56})$$

Adding Eqs. (A55) and (A56) gives

$$4 + 2\bar{x}_2(x_0 + y_0) = 0. \quad (\text{A57})$$

Thus $|x_0 + y_0| = 2$, the only possibility is

$$x_0 = y_0 = -x_2. \quad (\text{A58})$$

Applying Eqs. (A55)–(A58), we obtain $2\bar{x}_3 = 0$, which is a contradiction.

Case C2: $y_2 = x_4 \bar{x}_5$, $y_2 = -x_2$

First, we rewrite Eqs. (A2) and (A5) in terms of x_0 , x_2 , x_3 , x_4 , y_0 :

$$2x_3 \bar{x}_2 - 2\bar{x}_2 + x_0 + y_0 + x_4 \bar{x}_0 - x_4 \bar{y}_0 = 0, \quad (\text{A59})$$

$$2x_4 + 2x_4 \bar{x}_3 + x_0 \bar{x}_2 - y_0 \bar{x}_2 - \bar{x}_2 x_4 \bar{x}_0 - \bar{x}_2 x_4 \bar{y}_0 = 0. \quad (\text{A60})$$

If we have a valid solution $(x_2, x_3, x_0, y_0, x_4)$, it is easy to see that $(\xi^{-1} x_2, x_3, \xi x_0, \xi y_0, \xi^2 x_4)$ is also a valid solution for any unimodular complex number ξ . Therefore, we only need to consider the case $x_4 = 1$. Taking the conjugate of Eq. (A60), multiplying it by \bar{x}_2 , and letting $x_4 = 1$, Eqs. (A59) and (A60) give

$$2x_3 \bar{x}_2 - 2\bar{x}_2 + x_0 + y_0 + \bar{x}_0 - \bar{y}_0 = 0, \quad (\text{A61})$$

$$2x_3 \bar{x}_2 + 2\bar{x}_2 - x_0 - y_0 + \bar{x}_0 - \bar{y}_0 = 0. \quad (\text{A62})$$

Subtracting Eqs. (A62) and (A61), we obtain

$$4\tilde{x}_2 - 2(x_0 + y_0) = 0. \tag{A63}$$

Thus $|x_0 + y_0| = 2$, and the only possibility is

$$x_0 = y_0 = \tilde{x}_2. \tag{A64}$$

Applying Eqs. (A61)–(A64), we obtain $2x_3\tilde{x}_2 = 0$, which is a contradiction.

Case C3: $y_2 = x_4\tilde{x}_5, y_2 = -x_3x_4\tilde{x}_5$

This case is covered by Case A, because $x_3 = -1, y_3 = -x_3 = 1$.

Case C4: $y_2 = x_2, y_2 = -x_2$

This case is clearly not possible.

APPENDIX B: PROOF OF THEOREM 2

The proof follows a similar procedure to that of the proof of Theorem 1. The only difference is that the modulus of x_0, y_0 are changed from one to zero. Related changes in the proof in Appendix A are listed below.

Case A1: Eq. (A18) gives $2\tilde{x}_2 = 0$, which is a contradiction.

Case A2: Eq. (A24) gives $4\tilde{x}_2x_3 = 0$, which is a contradiction.

Case A3: Eq. (A32) gives $4\tilde{y}_2 = 0$, which is a contradiction.

Case A4: Eq. (A35) gives $2\tilde{x}_2 = 0$, which is a contradiction.

Case B1: Eq. (A43) gives $4 = 0$, which is a contradiction.

Case B4: Eq. (A49) gives $4x_2 = 0$, which is a contradiction.

Case C1: Eq. (A57) gives $4 = 0$, which is a contradiction.

Case C2: Eq. (A63) gives $4\tilde{x}_2 = 0$, which is a contradiction.

APPENDIX C: PROOF OF THEOREM 5

We prove the first part constructively. Using Eq. (18), we observe that it suffices to construct an aperiodic complementary array set. Without loss of generality, assume that $s = p_1^{q_1} \times p_2^{q_2} \cdots \times p_n^{q_n}$ is a prime factorization of s , where $q_j \geq 1$ and p_j 's are distinct for $j = 1, \dots, n$. Let $S^{(0)} = \{S_m^{(0)}\}_{m=1}^{p_1}$ be a set of p_1 sequences each of which contains a single point 1, i.e., $S^{(0)}$ has design parameters $(M, N, L) = (p_1, 1, 1)$.

In the first iteration, we apply Theorem 3 to $S^{(0)}$ with U equal to the Fourier matrix F_{p_1} while satisfying Remark 3 conditions to obtain a (one-dimensional) complementary array set with $(M, N, L) = (p_1, \text{lcm}(p_1, 1), p_1 \times 1) = (p_1, p_1, p_1)$. Applying Theorem 3 a second time, we obtain a complementary array set with $(M, N, L) = (p_1, \text{lcm}(p_1, p_1), p_1 \times p_1) = (p_1, p_1, p_1^2)$. After applying Theorem 3 to $S^{(0)}$ $q_1 - 1$ times, we obtain the complementary array set $S^{(1)}$ with $(M, N, L) = (p_1, p_1, p_1^{q_1-1})$.

In the second iteration, we first apply Theorem 4 to $S^{(1)}$ with $\tilde{M} = p_2$ while satisfying Remark 5 conditions. The resulting complementary array set has parameters $(M, N, L) = (p_2, \text{lcm}(p_1, p_2), p_1 \times p_1^{q_1-1}) = (p_2, p_1p_2, p_1^{q_1})$; then we apply Theorem 3 $q_2 - 1$ times with U being the Fourier matrix F_{p_2} to create the complementary array set $S^{(2)}$ with $(M, N, L) = (p_2, p_1p_2, p_1^{q_1}p_2^{q_2-1})$.

By recursive construction as above, after w th iteration we obtain the complementary array set $S^{(w)}$ with $(M, N, L) = (p_n p_1 \cdots p_w, p_1 \cdots p_w, p_1^{q_1} p_2^{q_2} \cdots p_n^{q_n})$. Finally, applying Theorem 3 with U equal to the Fourier matrix F_{p_n} an extra time to $S^{(w)}$,

we obtain a complementary array set with $(M, N, L) = (p_n p_1 p_2 \cdots p_w, p_1^{q_1} p_2^{q_2} \cdots p_n^{q_n})$. The proof of the second part is similar.

APPENDIX D: PROOF OF THEOREM 6

Let $\mathbb{Z}[\lambda]$ denote the polynomial ring over \mathbb{Z} , and $\Phi_N(\lambda)$ denote the N th cyclotomic polynomial. Let $\xi = \exp(i2\pi/N)$, $U_N = \{\xi^j | j = 0, \dots, N - 1\}$ be the group of N th roots of unity endowed with multiplication. For any $\eta \in U_N$, let $|\eta|$ denote the order of η in the cyclic group U_N . Because $\sum_{m=1}^M x_m = 0$, there exists a polynomial $F(\lambda) = \sum_{j=0}^{N-1} f_j \lambda^j \in \mathbb{Z}[\lambda]$ such that $f_j \geq 0$ and $F(\xi) = 0$.

We prove Theorem 6 using a sequence of lemmas.

Lemma 5 Let p_k be distinct prime numbers and integers $r_k > 0, k = 1, 2$. Then,

$$\Phi_{p_1}(\lambda^{p_1^{r_1-1} p_2^{r_2}}) = \prod_{i=0}^{r_2} \Phi_{p_1^{r_1} p_2^i}(\lambda), \tag{D1}$$

$$\Phi_{p_1}(\lambda^{p_1^{r_1-1} p_2^{r_2}}) = \Phi_{p_1}(\lambda^{p_1^{r_1-1} p_2^{r_2-1}}) \Phi_{p_1^{r_1} p_2}(\lambda), \tag{D2}$$

$$\Phi_{p_1}(\lambda^{p_1^{r_1-1}}) = \Phi_{p_1^{r_1}}(\lambda). \tag{D3}$$

Similar results hold if p_1 and r_1 are respectively replaced with p_2 and r_2 in the above equations.

Proof of Lemma 5:

Since both sides are monic and have degree $(p_1 - 1)p_1^{r_1-1} p_2^{r_2}$, it suffices to show that every zero of $\Phi_{p_1^{r_1} p_2^{r_2}}(\lambda)$ is a zero of $\Phi_{p_1}(\lambda^{p_1^{r_1-1} p_2^{r_2}})$. If η is a zero of $\Phi_{p_1^{r_1} p_2^{r_2}}(\lambda)$, then $|\eta| = p_1^{r_1} p_2^{r_2}$, which implies $|r p_1^{r_1-1}| = |\eta| / \text{gcd}(|\eta|, p_1^{r_1-1}) = p_1$. Therefore, η is also a zero of $\Phi_{p_1}(\lambda^{p_1^{r_1-1}})$.

The proof of Eqs. (D2) and (D3) is similar.

Lemma 6 If $n = 1$, i.e., $N = p_1^{r_1}$, then there exists a polynomial $A(\lambda) = \sum_{j=0}^{N/p_1-1} a_j \lambda^j \in \mathbb{Z}[\lambda]$, $a_j \geq 0$, such that

$$F(\lambda) = \Phi_{p_1}(\lambda^{N/p_1}) A(\lambda).$$

Proof of Lemma 6:

First, $\Phi_N(\lambda)$ divides $F(\lambda)$, because $F(\lambda)$ annihilates ξ and $\Phi_N(\lambda)$ is an irreducible and monic polynomial in the ring $\mathbb{Z}[\lambda]$. Besides this, Eq. (D3) gives $\Phi_{p_1}(\lambda^{N/p_1}) = \Phi_N(\lambda)$. Therefore, there exists a polynomial $A_k(\lambda) = \sum_{j=0}^{N/p_1-1} a_j \lambda^j \in \mathbb{Z}[\lambda]$ such that $F(\lambda) = \Phi_{p_1}(\lambda^{N/p_1}) A(\lambda)$.

Second, because $\text{deg}(F) < N$, we have $\text{deg}(A) = \text{deg}(F) - \text{deg}(\Phi_N(\lambda)) < p_1^{r_1-1} = N/p_1$. We note that $f_j = a_j, j = 0, \dots, N/p_1 - 1$ and that $f_j \geq 0$. Therefore, the coefficients of $A(\lambda)$ are nonnegative.

Lemma 7

If $n = 2$, i.e., $N = p_1^{r_1} p_2^{r_2}$, then there exist polynomials $\hat{A}_k(\lambda) \in \mathbb{Z}[\lambda], k = 1, 2$ such that

$$\hat{A}_1(\lambda) \Phi_{p_1}(\lambda^{N/p_1}) + \hat{A}_2(\lambda) \Phi_{p_2}(\lambda^{N/p_2}) = \Phi_N(\lambda). \tag{D4}$$

Proof of Lemma 7:

First, Eq. (D1) and its similar result (by replacing p_1, r_1 with p_2, r_2) imply that $\text{gcd}(\Phi_{p_1}(\lambda^{N/p_1}), \Phi_{p_2}(\lambda^{N/p_2})) = \Phi_N(\lambda)$.

Second, consider two polynomials $\hat{T}_{t_k}(\lambda) = 1 + \lambda + \dots + \lambda^{t_k-1}, k = 1, 2$, where $t_1 > t_2$ and $\text{gcd}(t_1, t_2) = 1$. We apply Euclidean division to t_1, t_2 to obtain $t_1 = t_2 q + b$,

$0 < b < t_2$. It is easy to observe that $T_{t_1}(\lambda) = T_{t_2}(\lambda) \sum_{j=1}^q \lambda^{t_1 - jt_2} + T_b(\lambda)$. If we continuously apply Euclidean division, we will find polynomials $\hat{A}_k(\lambda) \in \mathbb{Z}[\lambda]$, $k = 1, 2$ such that

$$\hat{A}_1(\lambda)T_{t_1}(\lambda) + \hat{A}_2(\lambda)T_{t_2}(\lambda) = 1. \quad (\text{D5})$$

Replacing t_1 , t_2 , and λ respectively by p_1 , p_2 , and $\lambda^{N/(p_1 p_2)}$ in Eq. (D5), multiplying both sides by $\Phi_N(\lambda)$, and using Eq. (D2) and its similar result, we obtain Eq. (D4).

Lemma 8

If $n = 2$, i.e., $N = p_1^{r_1} p_2^{r_2}$, then there exist polynomials $A_k(\lambda)$, $\deg(A_k) \leq N/p_k - 1$, $k = 1, 2$ such that $F(\lambda) = \sum_{k=1}^2 A_k(\lambda)H_k(\lambda)$, where $H_k(\lambda) = \Phi_{p_k}(\lambda^{N/p_k})$, $k = 1, 2$.

Proof of Lemma 8:

Clearly, $\Phi_N(\lambda)$ divides $F(\lambda)$ due to the reason mentioned before. Therefore, Lemma 7 implies that there exist polynomials $\hat{A}_k(\lambda) \in \mathbb{Z}[\lambda]$, $k = 1, 2$ such that $F(\lambda) = \sum_{k=1}^2 \hat{A}_k(\lambda)H_k(\lambda)$ holds.

It is easy to see that $\lambda^d H_k(\lambda)$ can be written as $\lambda^d H_k(\lambda) = (\lambda^N - 1)Q(\lambda) + \lambda^{d_0} H_k(\lambda)$ for some $Q(\lambda) \in \mathbb{Z}[\lambda]$, $0 \leq d_0 \leq N/p_k - 1$. Thus, there exist polynomials $A_k(\lambda)$, $\deg(A_k) \leq N/p_k - 1$, $k = 1, 2$, and $W(\lambda)$ such that

$$F(\lambda) = \sum_{k=1}^2 A_k(\lambda)H_k(\lambda) + W(\lambda)(\lambda^N - 1).$$

Since $\deg(F) \leq N/p_k - 1$, we obtain $W(\lambda) = 0$.

Lemma 9

The coefficients of $A_k(\lambda)$, $k = 1, 2$ in Lemma 8 can be made nonnegative.

Proof of Lemma 9:

Let

$$\begin{aligned} \mathfrak{D}_F &= \{[a_{10}, \dots, a_{1(N/p_1-1)}, a_{20}, \dots, a_{2(N/p_2-1)}] | F(\lambda) \\ &= \sum_{j_1=0}^{N/p_1-1} a_{1j_1} H_1(\lambda) + \sum_{j_2=0}^{N/p_2-1} a_{2j_2} H_2(\lambda)\}, \\ \mathfrak{D}_F^{(2)} &= \left\{ [a_{10}, \dots, a_{1(N/p_1-1)}, a_{20}, \dots, a_{2(N/p_2-1)}] | F(\lambda) \right. \\ &= \sum_{j_1=0}^{N/p_1-1} a_{1j_1} H_1(\lambda) + \sum_{j_2=0}^{N/p_2-1} a_{2j_2} H_2(\lambda), \\ &\left. a_{2j_2} \geq 0, \quad j_2 = 0, \dots, \frac{N}{p_2} - 1 \right\}. \end{aligned}$$

For a fixed integer $0 \leq j \leq N/p_1 - 1$, consider the set $\{j + kN/p_1, k = 0, \dots, p_1 - 1\} \bmod N$. For each $k = 0, \dots, p_1 - 1$, we apply Euclidean division to $j + kN/p_1$ and N/p_2 , and obtain integers $0 \leq g_k \leq N/p_2 - 1$, $0 \leq b_k \leq p_2 - 1$ such that $j + kN/p_1 = g_k + b_k N/p_2$. Because of the identity

$$\begin{aligned} &\bigcup_{\tau=0}^{p_2-1} \{g_k + (b_k + \tau)N/p_2, k = 0, \dots, p_1 - 1\} \\ &= \bigcup_{k=0}^{p_1-1} \{g_k + (b_k + \tau)N/p_2, \tau = 0, \dots, p_2 - 1\} \bmod N, \end{aligned}$$

within the set \mathfrak{D}_F we can always decrease $a_{1(j+\tau N/p_2 \bmod(N/p_1))}$, $\tau = 0, \dots, p_2 - 1$ by one, while increasing a_{2g_k} , $k = 0, \dots,$

$p_1 - 1$ by one. We conclude that the subset $\mathfrak{D}_F^{(2)}$ of \mathfrak{D}_F is not empty. To finish the proof, it suffices to show that within $\mathfrak{D}_F^{(2)}$, there exists an element with $a_{1j_1} \geq 0$ for all $j_1 = 0, \dots, N/p_1 - 1$. If this is not true, then there exists $\mu < 0$ such that

$$\mu = \max_{[a_{10}, \dots, a_{1(N/p_1-1)}, a_{20}, \dots, a_{2(N/p_2-1)}] \in \mathfrak{D}_F^{(2)}} \left\{ \min \left\{ a_{10}, \dots, a_{1\left(\frac{N}{p_1}-1\right)} \right\} \right\}. \quad (\text{D6})$$

Suppose that $a_{1j} = \mu$. For each $k = 0, \dots, p_1 - 1$, consider the nonnegative coefficient of the item λ^{j+kN/p_1} in $F(\lambda)$: $A_1(\lambda)H_1(\lambda)$ contributes a negative value a_{1j} to it, and thus $A_2(\lambda)H_2(\lambda)$ contributes a positive value. In other words, there exist integers $0 \leq g_k \leq N/p_2 - 1$, $0 \leq b_k \leq p_2 - 1$ such that $j + kN/p_1 = g_k + b_k N/p_2$ and that $a_{2g_k} > 0$. It is clear that g_k , $k = 0, \dots, p_1 - 1$ are distinct values. By similar reasoning as before, we can increase $a_{1(j+\tau N/p_2 \bmod(N/p_1))}$, $\tau = 0, \dots, p_2 - 1$ by one, while decreasing a_{2g_k} , $k = 0, \dots, p_1 - 1$ by one, in order to get another element in $\mathfrak{D}_F^{(2)}$. Thus, we can increase

$$\max_{[a_{10}, \dots, a_{1(N/p_1-1)}, a_{20}, \dots, a_{2(N/p_2-1)}] \in \mathfrak{D}_F^{(2)}} \left\{ \min \left\{ a_{10}, \dots, a_{1\left(\frac{N}{p_1}-1\right)} \right\} \right\},$$

contradicting the definition of μ in Eq. (D6).

Proof of Theorem 6:

Combining Lemmas 6–9, we conclude that $F(\lambda)$ can be written as

$$F(\lambda) = \sum_{k=1}^2 A_k(\lambda)H_k(\lambda),$$

$$\text{where } A_k(\lambda) = \sum_{j=0}^{N/p_k-1} a_{kj} \lambda^j \in \mathbb{Z}[\lambda], a_{kj} \geq 0,$$

$$H_k(\lambda) = \Phi_{p_k}(\lambda^{N/p_k}) = 1 + \lambda^{N/p_k} + \lambda^{2N/p_k} + \dots + \lambda^{(p_k-1)N/p_k},$$

which is equivalent to Eq. (22). Equation (23) then immediately follows from Eq. (22).

Acknowledgment. The authors thank Dr. Yaron Rachlin of the MIT Lincoln Laboratory for valuable comments and discussions.

REFERENCES

- W. Cook, M. Finger, T. Prince, and E. Stone, "Gamma-ray imaging with a rotating hexagonal uniformly redundant array," *IEEE Trans. Nucl. Sci.* **31**, 771–775 (1984).
- E. Caroli, J. Stephen, G. Di Cocco, L. Natalucci, and A. Spizzichino, "Coded aperture imaging in x-and gamma-ray astronomy," *Space Sci. Rev.* **45**, 349–403 (1987).
- N. Ohyama, T. Honda, and J. Tsujiuchi, "An advanced coded imaging without side lobes," *Opt. Commun.* **27**, 339–344 (1978).
- N. Ohyama, T. Honda, and J. Tsujiuchi, "Tomogram reconstruction using advanced coded aperture imaging," *Opt. Commun.* **36**, 434–438 (1981).
- Y.-W. Chen and K. Kishimoto, "Tomographic resolution of uniformly redundant arrays coded aperture," *Rev. Sci. Instrum.* **74**, 2232–2235 (2003).
- R. Simpson and H. H. Barrett, *Coded-Aperture Imaging* (Springer, 1980).
- E. E. Fenimore and T. Cannon, "Coded aperture imaging with uniformly redundant arrays," *Appl. Opt.* **17**, 337–347 (1978).
- D. J. Brady, D. L. Marks, K. P. MacCabe, and J. A. O'Sullivan, "Coded apertures for x-ray scatter imaging," *Appl. Opt.* **52**, 7745–7754 (2013).

9. N. Ohyama, T. Honda, J. Tsujiuchi, T. Matumoto, T. A. Inuma, and K. Ishimatsu, "Advanced coded-aperture imaging system for nuclear medicine," *Appl. Opt.* **22**, 3555–3561 (1983).
10. A. Busboom, H. D. Schotten, and H. Elders-Boll, "Coded aperture imaging with multiple measurements," *J. Opt. Soc. Am. A* **14**, 1058–1065 (1997).
11. M. J. Golay, "Point arrays having compact, nonredundant autocorrelations," *J. Opt. Soc. Am.* **61**, 272–273 (1971).
12. D. Calabro and J. K. Wolf, "On the synthesis of two-dimensional arrays with desirable correlation properties," *Inf. Control* **11**, 537–560 (1967).
13. T. Cannon and E. Fenimore, "A class of near-perfect coded apertures," *IEEE Trans. Nucl. Sci.* **25**, 184–188 (1978).
14. E. Fenimore, "Coded aperture imaging: predicted performance of uniformly redundant arrays," *Appl. Opt.* **17**, 3562–3570 (1978).
15. L. D. Baumert, *Cyclic Difference Sets* (Springer, 1971), Vol. **182**.
16. M. Finger and T. Prince, "Hexagonal uniformly redundant arrays for coded-aperture imaging," in *19th International Cosmic Ray Conference* (1985), Vol. **3**, pp. 295–298.
17. S. R. Gottesman and E. Fenimore, "New family of binary arrays for coded aperture imaging," *Appl. Opt.* **28**, 4344–4352 (1989).
18. K. Byard, "An optimised coded aperture imaging system," *Nucl. Instrum. Methods Phys. Res. Sect. A* **313**, 283–289 (1992).
19. A. Gourlay and J. B. Stephen, "Geometric coded aperture masks," *Appl. Opt.* **22**, 4042–4047 (1983).
20. S. Gottesman and E. Schneid, "Pnp-a new class of coded aperture arrays," *IEEE Trans. Nucl. Sci.* **33**, 745–749 (1986).
21. L. Fejes, "Über die dichteste kugellagerung," *Math. Z.* **48**, 676–684 (1942).
22. M. J. Golay, "Static multislit spectrometry and its application to the panoramic display of infrared spectra," *J. Opt. Soc. Am.* **41**, 468–472 (1951).
23. M. Golay, "Complementary series," *IRE Trans. Inf. Theory* **7**, 82–87 (1961).
24. J. Davis and J. Jedwab, "Peak-to-mean power control and error correction for OFDM transmission using Golay sequences and Reed-Muller codes," *Electron. Lett.* **33**, 267–268 (1997).
25. M. Parker, K. Paterson, and C. Tellambura, "Golay complementary sequences," in *Encyclopedia of Telecommunications* (Wiley, 2003).
26. S. Stanczak, H. Boche, and M. Haardt, "Are LAS-codes a miracle?" *Globecom* **1**, 589–593 (2001).
27. J. H. Choi, H. K. Chung, H. Lee, J. Cha, and H. Lee, "Code-division multiplexing based MIMO channel sounder with loosely synchronous codes and Kasami codes," in *64th Vehicular Technology Conference* (2006), pp. 1–5.
28. C. J. Colbourn, *CRC Handbook of Combinatorial Designs* (CRC Press, 2010).
29. M. Golay, "Note on complementary series," *Proc. IRE* **50**, 628–631 (1962).
30. R. J. Turyn, "Hadamard matrices, Baumert-Hall units, four-symbol sequences, pulse compression, and surface wave encodings," *J. Comb. Theory Ser. A* **16**, 313–333 (1974).
31. R. Craigen, W. Holzmann, and H. Kharaghani, "Complex Golay sequences: structure and applications," *Discrete Math.* **252**, 73–89 (2002).
32. K. G. Paterson, "Generalized Reed-Muller codes and power control in OFDM modulation," *IEEE Trans. Inf. Theory* **46**, 104–120 (2000).
33. A. Gavish and A. Lempel, "On ternary complementary sequences," *IEEE Trans. Inf. Theory* **40**, 522–526 (1994).
34. R. Craigen and C. Koukouvinos, "A theory of ternary complementary pairs," *J. Comb. Theory Ser. A* **96**, 358–375 (2001).
35. R. Craigen, S. Georgiou, W. Gibson, and C. Koukouvinos, "Further explorations into ternary complementary pairs," *J. Comb. Theory Ser. A* **113**, 952–965 (2006).
36. S. Budišin, "New complementary pairs of sequences," *Electron. Lett.* **26**, 881–883 (1990).
37. H. D. Luke, "Sets of one and higher dimensional Welch codes and complementary codes," *IEEE Trans. Aerosp. Electron. Syst.* **21**, 170–179 (1985).
38. M. Dymond, "Barker arrays: existence, generalization and alternatives," Ph.D. thesis (University of London, 1992).
39. E. Fenimore and G. Weston, "Fast delta Hadamard transform," *Appl. Opt.* **20**, 3058–3067 (1981).
40. F. J. MacWilliams and N. J. Sloane, "Pseudo-random sequences and arrays," *Proc. IEEE* **64**, 1715–1729 (1976).
41. L. Bomer and M. Antweiler, "Periodic complementary binary sequences," *IEEE Trans. Inf. Theory* **36**, 1487–1494 (1990).
42. L. Baumert, *Cyclic Difference Sets* (Springer, 1971).